Buffering of Genetic Regulatory Networks in *Drosophila melanogaster*

Justin M. Fear,*,† Luis G. León-Novelo,‡ Alison M. Morse,*,† Alison R. Gerken,*,† Kjong Van Lehmann,§ John Tower, Sergey V. Nuzhdin,**,1 and Lauren M. McIntyre*,†,1**

*Molecular Genetics and Microbiology and †Genetics Institute, University of Florida, Gainesville, Florida 32611, ‡Department of Biostatistics, University of Texas Health Science Center at Houston–School of Public Health, Houston, Texas 77030, §Memorial Sloan Kettering Cancer Center, New York, New York 10065, and **Molecular and Computational Biology Program, Dornsife College of Letters, Arts, and Sciences, University of Southern California, Los Angeles, California 90089

ORCID ID: 0000-0002-0077-3359 (L.M.M.)

ABSTRACT Regulatory variation in gene expression can be described by *cis*- and *trans*-genetic components. Here we used RNA-seq data from a population panel of *Drosophila melanogaster* test crosses to compare allelic imbalance (AI) in female head tissue between mated and virgin flies, an environmental change known to affect transcription. Indeed, 3048 exons (1610 genes) are differentially expressed in this study. A Bayesian model for AI, with an intersection test, controls type I error. There are ~200 genes with AI exclusively in mated or virgin flies, indicating an environmental component of expression regulation. On average 34% of genes within a cross and 54% of all genes show evidence for genetic regulation of transcription. Nearly all differentially regulated genes are affected in *cis*, with an average of 63% of expression variation explained by the *cis*-effects. *Trans*-effects explain 8% of the variance in AI on average and the interaction between *cis* and *trans* explains an average of 11% of the total variance in AI. In both environments *cis*- and *trans*-effects are compensatory in their overall effect, with a negative association between *cis*- and *trans*-effects in 85% of the exons examined. We hypothesize that the gene expression level perturbed by *cis*-regulatory mutations is compensated through *trans*-regulatory mechanisms, *e.g.*, *trans* and *cis* by *trans*-factors buffering *cis*-mutations. In addition, when AI is detected in both environments, *cis-mated*, *cis-virgin*, and *trans-mated–trans-virgin* estimates are highly concordant with 99% of all exons positively correlated with a median correlation of 0.83 for *cis* and 0.95 for *trans*. We conclude that the gene regulatory networks (GRNs) are robust and that *trans*-buffering explains robustness.

KEYWORDS transcription; genetic variation; *cis*- or *trans*-effects; allele-specific expression; *Drosophila*; regulatory mutations; purifying selection

DIFFERENCES in the level of expression between two alleles are widespread and play an important role in complex traits. They have been implicated in human disease phenotypes such as cancer and are an important component of variation in *Drosophila*, as well as yeast, plants, animals, and humans (Mendell and Dietz 2001; Brem *et al.* 2002; Cowles *et al.* 2002; Yan *et al.* 2002; Wittkopp *et al.* 2004, 2006, 2008b; Springer and Stupar 2007; Hutter *et al.* 2008; Smith and Kruglyak 2008; Tirosh *et al.* 2009; Emerson *et al.* 2010; McManus *et al.* 2010; Crowley *et al.* 2015). In *Drosophila*, variation in gene expression is heritable (Wayne *et al.* 2004, 2007) and evidence for both *cis*- and *trans*-regulatory polymorphisms is widespread (Wittkopp *et al.* 2004, 2008b; Hughes *et al.* 2006; Genissel *et al.* 2008; Wang *et al.* 2008; Graze *et al.* 2009, 2012, 2014) and evidence for *cis*- by *trans*-interactions has been reported (Wittkopp *et al.* 2004, 2008b; Wang *et al.* 2008; Graze *et al.* 2014). It has been argued that these interactions may also present evidence for coevolution of *cis*- and *trans*-regulation between species (Wittkopp *et al.* 2004).

A variety of genetic designs have been used to identify *cis*- and *trans*-effects, including chromosome substitution (Hughes *et al.* 2006; Lemos *et al.* 2008; Wang *et al.* 2008; Wittkopp *et al.* 2008a; Graze *et al.* 2014), expression QTL

doi: 10.1534/genetics.116.188797
Manuscript received March 2, 2016; accepted for publication May 17, 2016; published Early Online May 18, 2016.
Supplemental material is available online at www.genetics.org/lookup/suppl/doi:10.1534/genetics.116.188797/-/DC1.
[1]Corresponding authors: 1376 Mowry Rd., CG Research Bldg., University of Florida, Gainesville, FL 32607. E-mail: mcintyre@ufl.edu; and Molecular and Computational Biology Program, Dornsife College of Letters, Arts, and Sciences, University of Southern California, Los Angeles, CA 90089. E-mail: snuzhdin@usc.edu

(eQTL) (reviewed by Brem *et al.* 2002; Kirst *et al.* 2005; Genissel *et al.* 2008; Gilad *et al.* 2008; Mackay *et al.* 2009; King *et al.* 2012, 2014; Massouras *et al.* 2012), and allelic imbalance (reviewed by Yan *et al.* 2002; Lo *et al.* 2003; Wittkopp *et al.* 2004, 2008a,b; Ronald *et al.* 2005; Guo *et al.* 2008a; Graze *et al.* 2009, 2012; Tirosh *et al.* 2009; Zhang and Borevitz 2009; McManus *et al.* 2010; Pastinen 2010). While eQTL studies often refer to *cis*- and *trans*-effects, eQTL *cis*-effects are local effects and *trans*-effects are distal effects (Rockman and Kruglyak 2006). In contrast, the *cis*- and *trans*-effects in allelic imbalance (AI) studies refer to molecular effects in the regulatory region of the locus itself (*cis*) or variation in genes molecularly interacting with common regulatory elements (*trans*) (Figure 1) (Yan *et al.* 2002; Wittkopp *et al.* 2004; Graze *et al.* 2009, 2012; Wittkopp and Kalay 2012).

Previous studies of AI in *Drosophila* examining interspecies hybrids (Michalak and Noor 2003, 2004; Ranz *et al.* 2004; Wittkopp *et al.* 2004; Ortiz-Barrientos *et al.* 2007; Graze *et al.* 2009; McManus *et al.* 2010, 2014; Graze *et al.* 2012) identified *cis*-effects in 20–90% of genes (Wittkopp *et al.* 2004; Graze *et al.* 2009, 2012; McManus *et al.* 2014; Meiklejohn *et al.* 2014). Most intraspecific studies have used chromosomal substitutions and these studies have found contributions of *trans*-effects ranging from 0.01% (McManus *et al.* 2014) to 40–50% of genes (Wittkopp *et al.* 2004; Meiklejohn *et al.* 2014) but sometimes reaching 90% of genes (Wang *et al.* 2008).

In a single hybrid, *cis*-regulatory variation is identified by comparing gene expression of two alleles at the same loci within that hybrid genotype (reviewed by Pastinen 2010) while *trans*-estimates are derived from comparing the same allele between hybrid genotypes (Figure 1). For a single hybrid, the estimates of *cis* are confounded with *cis*- by *trans*-interactions, and interactions are usually assumed to be negligible relative to the main effect of *cis*. When multiple genetically variable lines are crossed to a common tester line, *cis*- and *trans*-effects for each allele in the population can be estimated relative to the effects of the common tester allele (Nuzhdin *et al.* 2012). By modeling AI as a function of *cis* and *trans* and their interaction in the population, the contribution of these effects to AI can be estimated.

Identifying genes where AI occurs is a critically important biological problem, yet successfully identifying AI is technically challenging. Whereas mapping to a common reference strain is convenient, it introduces bias in the assessment of AI due to the difference in polymorphisms between the alleles interrogated and the reference (Degner *et al.* 2009; Graze *et al.* 2012). Masking SNPs and extensive filtering may ameliorate some sources of potential bias (Stevenson *et al.* 2013; van de Geijn *et al.* 2014), but bias may come from multiple sources and not all of these can be effectively filtered (Degner *et al.* 2009; Leon-Novelo *et al.* 2014; van de Geijn *et al.* 2014). There is mounting evidence that using personal genomes is more effective at reducing bias, particularly from structural variants (Degner *et al.* 2009; Rozowsky *et al.* 2011; Graze *et al.* 2012; Yuan and Qin 2012; Munger *et al.* 2014; Zou *et al.* 2014). Further, previously unidentified structural variation can be identified and the bias corrected using appropriate DNA controls (reviewed by Wittkopp *et al.* 2004; Pastinen 2010; Graze *et al.* 2012) and it is impossible to detect and filter such bias without DNA controls. This is often ignored, yet small amounts of unaccounted for bias lead to gross inflation of type I error rates (Leon-Novelo *et al.* 2014). Bias correction remains an important, and mostly ignored, feature of testing for AI.

The extent to which regulation of expression is sensitive to the environment is an interesting and not fully resolved issue. A frequent lack of concordance between eQTL across environments or genetic backgrounds has been previously interpreted as strong evidence for differential gene regulation in *Drosophila* (Mackay *et al.* 2009; Massouras *et al.* 2012; Huang *et al.* 2015). However, eQTL are reproduced between homozygous and heterozygous flies (Massouras *et al.* 2012), and regulatory variation measured using allelic imbalance appeared robust to environmental perturbations in *Arabidopsis* (Cubillos *et al.* 2014). Here, we have assayed the transcriptome in virgin and mated flies to test whether AI variation responds to mating.

Following mating in *Drosophila melanogaster* the fly experiences changes in metabolism (McGraw *et al.* 2004, 2008; Dalton *et al.* 2010), immune defense (reviewed by Lawniczak and Begun 2004; Peng *et al.* 2005; Lawniczak *et al.* 2007; Morrow and Innocenti 2012), life span (Chapman *et al.* 1995), detoxification products (McGraw *et al.* 2004), and gene expression (Smith *et al.* 2013; Zhou *et al.* 2014). Metabolic changes are found throughout the whole body (McGraw *et al.* 2004, 2008) as well as specific changes in the female head fat body (Dalton *et al.* 2010), including effects on nutritional state postmating.

This study explores whether an allelic imbalance in an interspecific population of *D. melanogaster* differs by environment and whether regulatory variation equally involves *cis*- and *trans*-effects. Consistent with the literature, this study finds 54% of all genes have evidence for AI. Coevolutionary processes between species result in *cis*- by *trans*-interactions, which have been clearly demonstrated in *melanogaster/simulans* hybrids (Wittkopp *et al.* 2004, 2008b; Landry *et al.* 2005; Graze *et al.* 2009, 2012; Fontanillas *et al.* 2010; Stevenson *et al.* 2013; McManus *et al.* 2014). However, coevolution is not a plausible explanation within species. We propose an alternative hypothesis for apparent *cis–trans* compensation, where the gene expression level perturbed by *cis*-regulatory mutations is partially compensated through *trans*-regulatory mechanisms. This is supported by recent experimental evidence of widespread molecular interactions as a result of cryptic genetic variation (Paaby and Rockman 2014).

Methods

All original data are attached to this article in File S1 and described in the Supplemental Material. All programs used

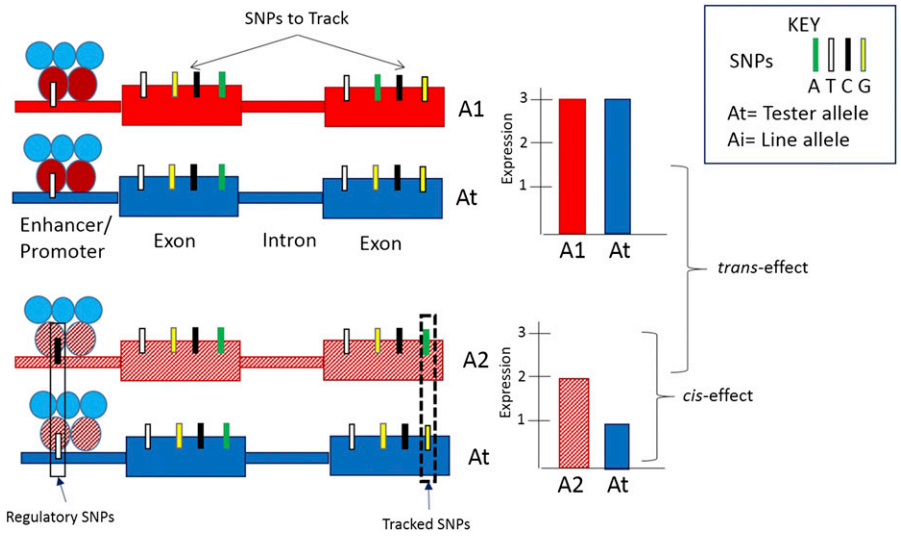

Figure 1 Cartoon of *cis*- and *trans*-regulation. A1 and A2 are alleles from two different testcrosses of a parental line (A1, red; A2, cross-hatched red) with a tester allele (At, blue). Alleles are tracked by SNPs within the coding sequence. Note that these SNPs are not necessarily causal. For testcross 1, there is no allelic imbalance; allele-specific expression is equal between the A1 allele and the At allele. For testcross 2, the A2 allele is different from the At allele, indicating *cis*-regulation. In this cartoon, the expression of the exon is regulated by a regulatory SNP within the gene's promoter. *Trans*-effects are identified by comparing the expression of the At allele in testcross 1 to the expression of the At allele in testcross 2.

for analysis, plus documentation, are at http://github.com/McIntyre-Lab/papers/tree/master/fear_ase_2016.

Sequencing data

RNA-seq data from a panel of 68 *D. melanogaster* F_1 hybrids (Kurmangaliyev *et al.* 2015) were used to measure allele-specific expression. Briefly, females from two populations of naturally derived *D. melanogaster* strains [54 from the *Drosophila* Genetic Reference Panel (DGRP) (Mackay *et al.* 2012) and 14 from Winters, California] were crossed to males of a single *D. melanogaster* laboratory strain (w^{1118}). Kurmangaliyev *et al.* (2015) isolated RNA from pools of ~50 adult female heads from the F_1 hybrid progeny. At least 3 independent biological replicates of each cross were evaluated. Libraries were constructed using standard protocols and pooled at equal molar concentrations. They were sequenced in eight or more lanes of Illumina HiSeq 2000. FlyBase v5.51 was used and exons were identified from this build. Exons that overlapped within a gene were collapsed as in Graze *et al.* (2012).

Genome ambiguity: simulation 1 random SNPs

Genome ambiguity is a major source of mapping bias (Degner *et al.* 2009), but it can be estimated via simulation (Degner *et al.* 2009; Leon-Novelo *et al.* 2014). To identify regions of genome ambiguity we simulated data similar to the intraspecific hybrid population studied here. On average, parental genotypes have ~160,000 exonic SNPs compared to the reference (FlyBase v5.51). Parental genotypes for 101 lines were simulated by randomly incorporating 160,000 SNPs into 63,181 exons of the *D. melanogaster* reference (FlyBase v5.51). All possible 95-bp reads were created from each reference, using a sliding window. An F_1 panel ($n = 100$) was constructed by taking simulated reads from each of 100 simulated genotypes ($line_i$ where $i = 1$–100) and mixing them with a single common simulated genotype ($line_i$: tester). Reads were aligned to each "parental" reference ($line_{101}$: tester), using Bowtie (v0.12.9, -m1, -v3) (Langmead *et al.* 2009) and Last (v247, -l 25) (Frith *et al.* 2010). Genotype-specific alignments were compared as in Graze *et al.* (2012) and reads were categorized as aligning best to the "line" or the "tester' or aligning equally well to "both." For each exon, bias (q) was estimated by taking the proportion of reads that aligned to the tester over the sum of the allele-specific reads ($line_i$ + tester). Because the simulated F_1 panel was created by equally mixing reads from parental strains, q is expected to be 0.5. When q deviates from 0.5, the exons must contain sequence ambiguities that affect the mappability of this region. A total of 55,647 exons showed no sequence ambiguity, while 7534 have some evidence of ambiguity (Table S1). Of these there were 1372 that were ambiguous in >50% of simulated lines, and 807 were ambiguous in all 100 simulated F_1 hybrids (Figure S1A). We removed the 807 exons that were ambiguous in all lines from the remainder of analyses.

Genotype-specific references

Genotype-specific references have been used to reduce map bias (Degner *et al.* 2009; Rozowsky *et al.* 2011; Graze *et al.* 2012; Yuan and Qin 2012; Stevenson *et al.* 2013; Leon-Novelo *et al.* 2014; Munger *et al.* 2014) by incorporating a filtered set of SNPs and indels that were identified in each parental strain. The GATK UnifiedGenotyper tool (ver. 2.1-8) was used to identify SNPs and indels in 68 genotypes (DGRP and Winters; line) and the laboratory strain (w^{1118}; tester). To minimize biases from miscalled variants (Leon-Novelo *et al.* 2014), SNPs and indels were strictly filtered as follows. All variants were considered as a line–tester pair, and if a variant was heterozygous in either the line or the tester, it was removed. The remaining SNP locations were masked in the genomic reference (FlyBase r5.51) for each line–tester pair ($n = 68$), by replacing the current nucleotide with an "N". RNA-seq data from each F_1 hybrid were aligned to the masked reference, using Bowtie (v0.12.9, -a, -v3) (Langmead *et al.* 2009) followed by Last (v247, -l 25) (Frith *et al.* 2010). A custom python script summarized masked alignment files by counting the number of RNA-seq reads that supported

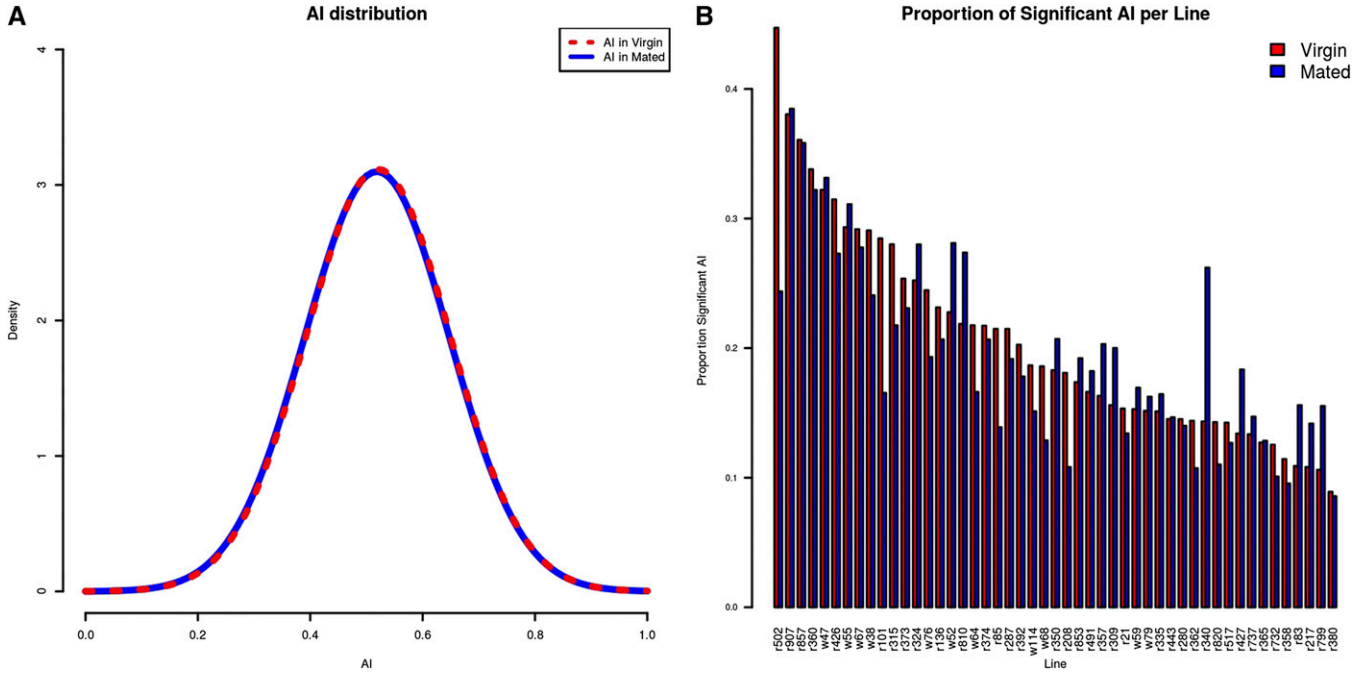

Figure 2 Distribution of AI. (A) Distribution of $\hat{\theta}$ for mated (blue) and virgin (red) environments for all data. The distribution is centered at 0.5, indicating that there is no overall bias toward the line or the tester allele. (B) The proportion (*y*-axis) of exons significant for AI, determined by the intersection test, for each line (*x*-axis) in mated (blue) and virgin (red) environments.

each variant call (*SNP* or *indel*). A variant (SNP or indel) was retained if it had at least one supporting RNA-seq read or if the DNA coverage for the original variant call was five or more. Filtered variants (File S1) were used to create a genotype-specific exome reference by updating the *D. melanogaster* genomic reference (FlyBase r5.51) with SNPs and indels and removing redundant exons.

Genotype-specific bias estimation: simulation 2 (qSIM)

Previous studies have used DNA read counts to estimate inherent bias and then corrected these biases by including a random effect parameter in their allelic imbalance models (Wittkopp *et al.* 2004; Graze *et al.* 2012; Leon-Novelo *et al.* 2014). Here we do not have DNA read counts; however, we use read simulation to identify exons that contain ambiguity and to create a bias correction parameter (q = qSIM; see Leon-Novelo *et al.* 2014). To mimic the information provided by the DNA, we simulated all possible 95-bp DNA reads from each parental genotype-specific exome reference (DGRP, Winters, and w^{1118}) (see *Methods*: *Genotype-specific references*). Similar to genome ambiguity simulation, a hybrid was created by mixing reads from each line (n = 49) with reads from the common laboratory strain (w^{1118}). Simulated hybrid reads were aligned separately to the line and tester genotype-specific references, using Bowtie (v0.12.9, -m1, -v3) (Langmead *et al.* 2009) and Last (v247, -l 25) (Frith *et al.* 2010). Genotype-specific alignments were compared as in Graze *et al.* (2012) and reads were categorized as aligning best to the line or the tester or aligning equally well to both. For each exon, the bias term (qSIM) was calculated by taking the proportion of reads that aligned to the tester over the sum of the allele-specific reads (line_i + tester). After removing 807 exons that are always biased in genome ambiguity simulations (see *Methods*: *Genome ambiguity: simulation 1 random SNPs*), 53,923 exons showed no bias (qSIM = 0.5), while 8451 regions showed bias in at least 1 line–tester combination (Figure S1B and Table S1). The bias with the biggest difference from 0.5 was used as the estimate for bias for each exon.

Mapping

Genotype-specific references were created by updating the genome, using variants identified by global alignments of these and all other data for *D. melanogaster* lines simultaneously (Table S2). Data for the 68 lines were mapped to each parent and w^{1118} separately to the line and tester genotype-specific references, using Bowtie (v0.12.9, -m1, -v3) (Langmead *et al.* 2009) and Last (v247, -l 25) (Frith *et al.* 2010). Reads in exons were counted and classified as aligning to the line, to the tester, or to both. Several filtering steps were performed. Exons that always showed bias in the genome ambiguity simulation were removed. Exons with very low coverage (average per nucleotide coverage <25) were removed (n = 31,791). Exons that were not present in at least 10% of genotypes were removed (n = 11,382). Exons that were not present in both environments (virgin, mated) were removed (n = 1253; 5391 remaining). After filtering exons, genotypes whose median value across all lines (for the ratio of tester-specific to total allele-specific read counts) was extreme ($\leq$0.4 or $\geq$0.6) were removed (n = 9) as these likely

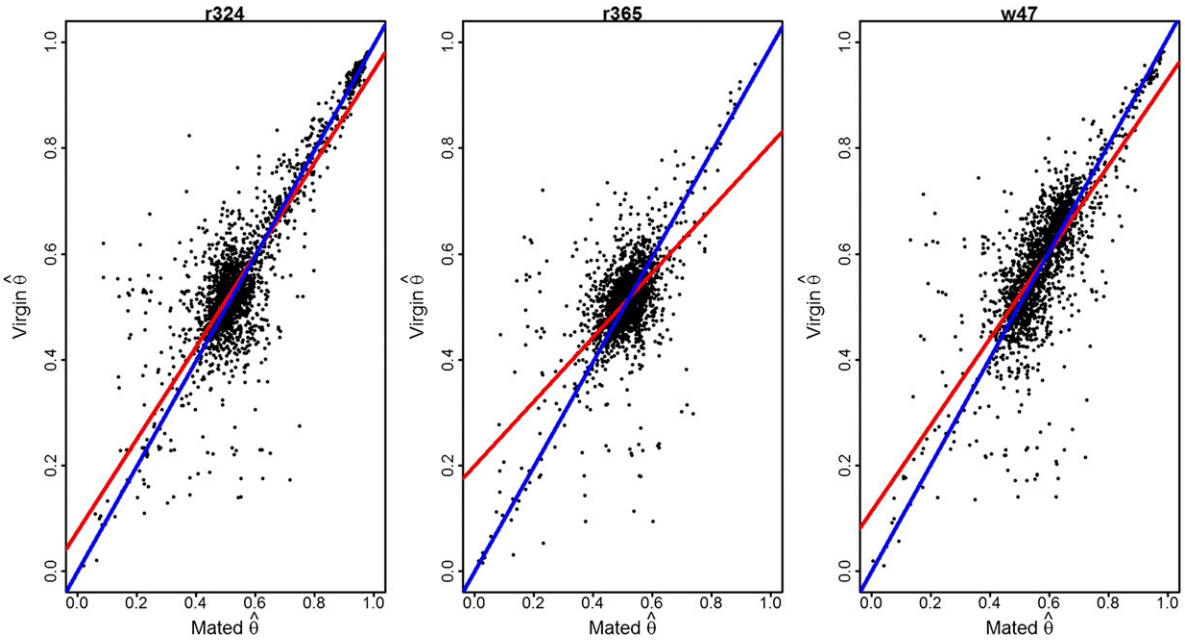

Figure 3 Estimates of AI in the mated *vs.* virgin environment. Three lines (r324, r365, and w47) were selected at random. $\hat{\boldsymbol{\theta}}$ for the mated environment (*x*-axis) and the virgin environment (*y*-axis) for all exons was evaluated. Each exon is a point on the graph. Estimates of AI are remarkably similar between mated and virgin environments. The red line in the panels is a regression while the blue line has an intercept of (0, 0).

reflect poor variant detection and systematic bias. Finally, genotypes with <500 remaining exons were removed (n = 13). A total of 49 genotypes and 5391 exons were analyzed for allelic imbalance (File S2).

An intersection test for AI

We use the Poisson Gamma (PG) model developed by Leon-Novelo *et al.* (2014). Briefly, under the null hypothesis of no allelic imbalance $H_0: \theta = 0.5$ *vs.* the alternative of allelic imbalance $H_1: \theta \neq 0.5$. Let x_i and y_i be the line and tester RNA allele-specific read counts in biological replicate $i(i = 1, \ldots I)$:

$$y_i|\, \mu, \alpha, \beta_i, q \;\sim\; \text{Poisson}(\mu\alpha\beta_i q),$$

and

$$x_i|\;\; \mu, \beta_i, q \;\sim\; \text{Poisson}\big(\mu\beta_i(1-q)\big).$$

Here μ is the overall mean, β_i is the variation of biological replicates $(i = 1, \ldots, I)$, α is the effect of a read having AI, and q is a constant to incorporate bias information, where values >0.5 indicate bias toward the tester allele and values <0.5 are bias toward the line allele. If θ is the real proportion of reads from the tester allele, then

$$\theta = \frac{\mu\alpha\beta_i}{\mu\beta_i + \mu\alpha\beta_i} = \frac{\alpha}{1+\alpha}.$$

When there is no AI ($\theta = 0.5$), therefore $\alpha = 1$. The bias correction parameter q can either be a fixed constant (*e.g.*, 0.5) or be a random variable. The PG model requires that exons have at least three biological replicates for a given genotype × mating status and that the exon is expressed in at least one of these replicates (*i.e.*, average per nucleotide coverage >0). For those exons where qSIM captures the potential bias this value is used in the Bayesian model. The simulated value of qSIM, when different from 0.5, has been shown to reflect bias from DNA controls and to be close to the value of bias estimated from DNA (Leon-Novelo *et al.* 2014). Note that the input to this model is raw read counts and that no additional normalization is performed.

The type I error rate for this test is <5% only when there is modest misspecification of bias; however, error rate increases as the percentage of misspecification increases (Leon-Novelo *et al.* 2014). For the commonly used binomial procedure in the test for AI type I error rates are large (Degner *et al.* 2009; Fontanillas *et al.* 2010; Nothnagel *et al.* 2011; Yuan and Qin 2012; Leon-Novelo *et al.* 2014; van de Geijn *et al.* 2014; Zou *et al.* 2014; Castel *et al.* 2015). Using DNA controls to estimate bias reveals that most bias (95%) is <20% (Graze *et al.* 2012). This translates to values of the parameter q between 0.4 and 0.6. Evaluating the posterior at three values of q, 0.4, 0.5, and 0.6, provides an estimate of the behavior of the posterior for the most likely set of conditions. Using an intersection test approach (Stell *et al.* 1980; Berger 1997; Berger and Boos 1999; Coffman *et al.* 2003), AI is declared if the credible interval excludes 0.5 for all three values of q.

The type I error behavior of the proposed intersection test was evaluated using simulation. Read counts for 10,000 genes were simulated using a Poisson distribution. The Poisson model was parameterized similarly to the above AI PG model: with mean read counts estimated from the population panel for three classes of coverage (low, medium, and high), the bias

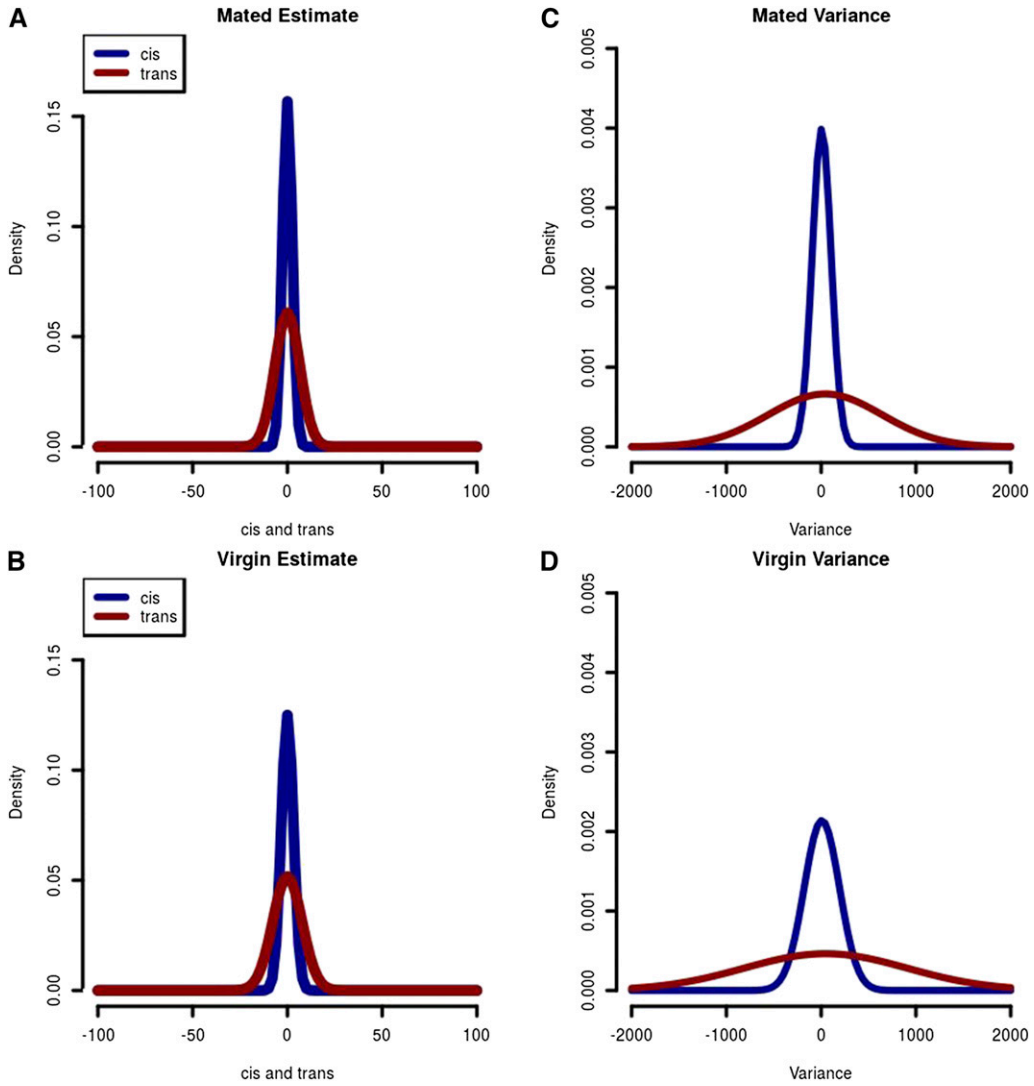

Figure 4 Distribution of *cis* and *trans* for exons with significant AI. (A) Distribution of estimates of *cis* and *trans* for the mated environment. *Trans*-estimates appear to have a larger variance than the *cis*-estimates. *Cis* and *trans* are centered at zero, as expected. (B) Distribution of estimates of *cis* and *trans* for the virgin environment. *Trans*-estimates appear to have a larger variance than the *cis*-estimates. *Cis* and *trans* are centered at zero, as expected. (C) Distribution of the variance for *cis*- and *trans*-estimates for the mated environment. For each exon, the variance of the estimate is calculated. The variance in *trans*-estimates can be much larger than the variance in *cis*-estimates. (D) Distribution of the variance for *cis*- and *trans*-estimates for the virgin environment. For each exon, the variance of the estimate is calculated. The variance in *trans*-estimates can be much larger than the variance in *cis*-estimates.

varied from 0.35 to 0.65 (19 values altogether), and all simulations were the null case (no AI). For each level of bias simulated, the simulated bias was used in the model and several deviations from the simulated bias, misspecification, were evaluated (1%, 2%, 3%, 5%, 10%, and 20%). For each combination of bias and misspecification (19×6) the posterior distribution of θ was estimated using the above AI PG model and intersection test ($q = [0.4, 0.5, 0.6]$). Note that the simulation is performed in relative bias amounts and not absolute. For example, 10% of 0.4 is 0.04 and 10% of 0.6 is 0.06. This was done for demonstration purposes, as the direction of the AI is arbitrary and this reveals more about the behavior of the bias.

Estimation of cis- and trans-effects

With the tester-cross design, allele-specific read counts can be used to separate *cis*- and *trans*-effects (Nuzhdin *et al.* 2012). For the sake of clarity in this article the reasoning in Nuzhdin *et al.* (2012) is reproduced here. In the testcross, the expression of the population allele i and the tester allele t in genotype i can be expressed as

$$E_{ii} = \mu + C_i + \frac{T_i + T_t}{2} Line$$

$$E_{ti} = \mu + C_t + \frac{T_i + T_t}{2} Tester,$$

where μ is the population mean, C_i is the *cis*-effects of allele i, T_i is the *trans*-effects of the allele i, and T_t is the *trans*-effects of the tester allele. Several constraints are necessary to solve this system. For simplicity assume $\sum_{i=1}^{n} C_i = 0$ and $\sum_{i=1}^{n} T_i = 0$. The expected difference between the alleles over the population is $\sum_{i=1}^{n}((E_{ti} - E_{ii})/n)$, which is equivalent to $\sum_{i=1}^{n}((C_t - C_i)/n) = C_t$. The tester *trans*-effects are estimated by $T_t = 2 \times \left(\sum_{i=1}^{n} E_{ti}/n - \mu - C_t\right)$, which is $-C_t$. The *cis*-effects for each allele are estimated as $C_i = E_{ii} - E_{ti} + C_t$. The line *trans*-effects are estimated by $T_i = 2 \times (E_{ti} - \mu - C_t) - T_t$. This formulation assumes equal coverage across lines. To account for the varying number of reads and the varying specificity of each cross, allelic expression was scaled to the number of non-allele-specific reads in the same region. That is, E_{ii} is estimated as the number of reads mapping uniquely

to allele i divided by the number of reads mapping to the region but not assignable to allele i or the tester allele. Without scaling, the estimation is reflective only of the relative number of reads for that cross. In addition, this is a system of four unknowns and two equations, meaning there is not a unique solution for all four effects. The effects of C_t and T_t in this design are confounded with each other and will vary, depending on the exact estimation strategy for the population mean. However, the estimation of the effects C_i and T_i is not sensitive to the strategy for estimation of the population mean.

Data availability

The authors state that all data necessary for confirming the conclusions presented in the article are represented fully within the article.

Results

Allele-specific expression was compared between 49 test-crosses of females that were either mated or virgin. F_1 hybrids were produced between a w^{1118} tester strain and genotypes from the DGRP and a Winters collection (Campo *et al.* 2013). We use a Bayesian test for AI that accounts for bias and controls type I errors (Figure S2). The ability to detect AI is related to coverage. Exons with allelic imbalance were underrepresented in genotypes with low levels of coverage (Table S2) of fewer than three reads per nucleotide. AI is concordant across the length of the transcript with very few ($n = 82$) exceptions (Table S3). These genes show AI in two or more exons in different directions, with at least one exon with more expression in the line and at least one other exon with more expression from the tester allele. The few differences across the gene may represent a frequency difference in isoform usage between alleles (Kurmangaliyev *et al.* 2015) and are consistent with data observed in other species (Skelly *et al.* 2011; Anders *et al.* 2012; Trapnell *et al.* 2013).

As with previous studies (Lawniczak and Begun 2004; McGraw *et al.* 2004, 2008; Mack *et al.* 2006; Kocher *et al.* 2008; Dalton *et al.* 2010; Smith *et al.* 2013) there is substantial difference in expression between virgin and mated flies. We observed 3048 exons from 1610 genes exhibiting differential expression at a false discovery rate of 0.05 (Benjamini and Hochberg 1995). In addition, 7 of the top 10 genes were reported previously in an analysis of gene expression in the heads of virgin and mated flies, which provides support for the present results (Dalton *et al.* 2010).

Of the 5391 exons analyzed, 4090 (76%) showed evidence of allelic imbalance in at least 1 cross. Fourteen regions had AI in >40 crosses (of 49 total), and 31 regions had AI in 100% of the crosses measured. The few that are different in all crosses likely result from regulatory mutations unique to the w^{1118} strain. There were 3004 exons that had AI in ≤5 crosses, and 570 exons showed AI in <5 crosses. The distribution of θ is centered on 0.5 for both mated and virgin environments (Figure 2A). An average of 19% of exons show evidence for AI in any one cross. The proportion of exons with significant AI ranged from 8% of exons tested to 39% (Figure 2B and Table S3). Of the exons with allelic imbalance, one-third are also differentially expressed between environments.

Table 1 Direction of *cis*- and *trans*-effects

	Direction *trans*		
Direction *cis*	+	−	Total
+	9,090	22,300	31,390
−	11,869	10,621	22,490
Total	20,959	32,921	53,880

If the value of the estimate is positive, the direction is recorded as (+); similarly negative values are scored as (−). The direction of *cis*-effects is compared to the direction of *trans*-effects. There are (9090 + 10,621) *cis*- and *trans*-estimates that are concordant and (22,300 + 11,869) *cis*- and *trans*-estimates that are compensatory.

Environmental effects on allelic imbalance

We looked to see whether there were any differences in AI between mated and virgin flies. The exons that show differences in estimates of allelic imbalance between mated and virgin flies are listed in Table S4. There were 93 genes that were significant in AI in mated flies only. Several genes associated with reproduction were significant for AI in mated flies only, including *Arpc1*, *CG10433*, *CG17919*, *fry*, *heph*, *Sec5*, *Cg25C*, and *Shark*. Mating has been shown to reduce life span (Chapman *et al.* 1995; Flatt 2011; Landis *et al.* 2015) and several genes reported to affect life span were also significant for AI in mated flies only (*α-Man-Ia*, *bmm*, *mt:ATPase6*, *sNPF*, and *sm*). Postmating immunity is also compromised in female fruit flies (reviewed by Peng *et al.* 2005; Lawniczak *et al.* 2007; McGraw *et al.* 2008) and the genes *CG10433*, *CG17652*, *CG17919*, *Gs1l*, *α-Man-Ia*, *mtd*, *Sec5*, and *Shark* are involved in processes such as apoptosis, phagocytosis, and general immune responses. In addition, *Cyp4ac1*, *bmm*, *Gs1l*, and *sNPF* are associated with metabolism, which is also altered by mating in fruit flies (McGraw *et al.* 2004, 2008; Dalton *et al.* 2010; Zhou *et al.* 2014).

Interestingly, there were two genes that have been shown to be directly involved in regulatory regions of the genome that were significant for AI in mated flies. *cha* is involved in cholinergic neuronal regulation and *cis*-regulation in the brain (Yasuyama *et al.* 1995). *cnc* encodes the *Drosophila* homolog of the Nrf2 transcription factor that is directly linked to metabolic regulation, stress response (Misra *et al.* 2011; Sykiotis *et al.* 2011; Pickering *et al.* 2013), and life span (Obata and Miura 2015). *cnc* has a direct influence on the oocyte nucleus and gurken, signaling (Guichet *et al.* 2001) innate immunity and lipid metabolism (Karim *et al.* 2015), and its overexpression can restore movement in a *Drosophila* model of Parkinson's disease (Barone *et al.* 2011).

In virgin flies, there were 99 genes that were significant for AI. Reproductive-related activities were also represented in virgins as they were in mated flies (*Cdc42*, *Cys*, *dnc*, *fl(2)d*, *mei-P26*, *qm*, and *zip*). In addition, *Tim10*, a negative regulator of innate immune response, was also significant in AI in virgin females only, suggesting that upon

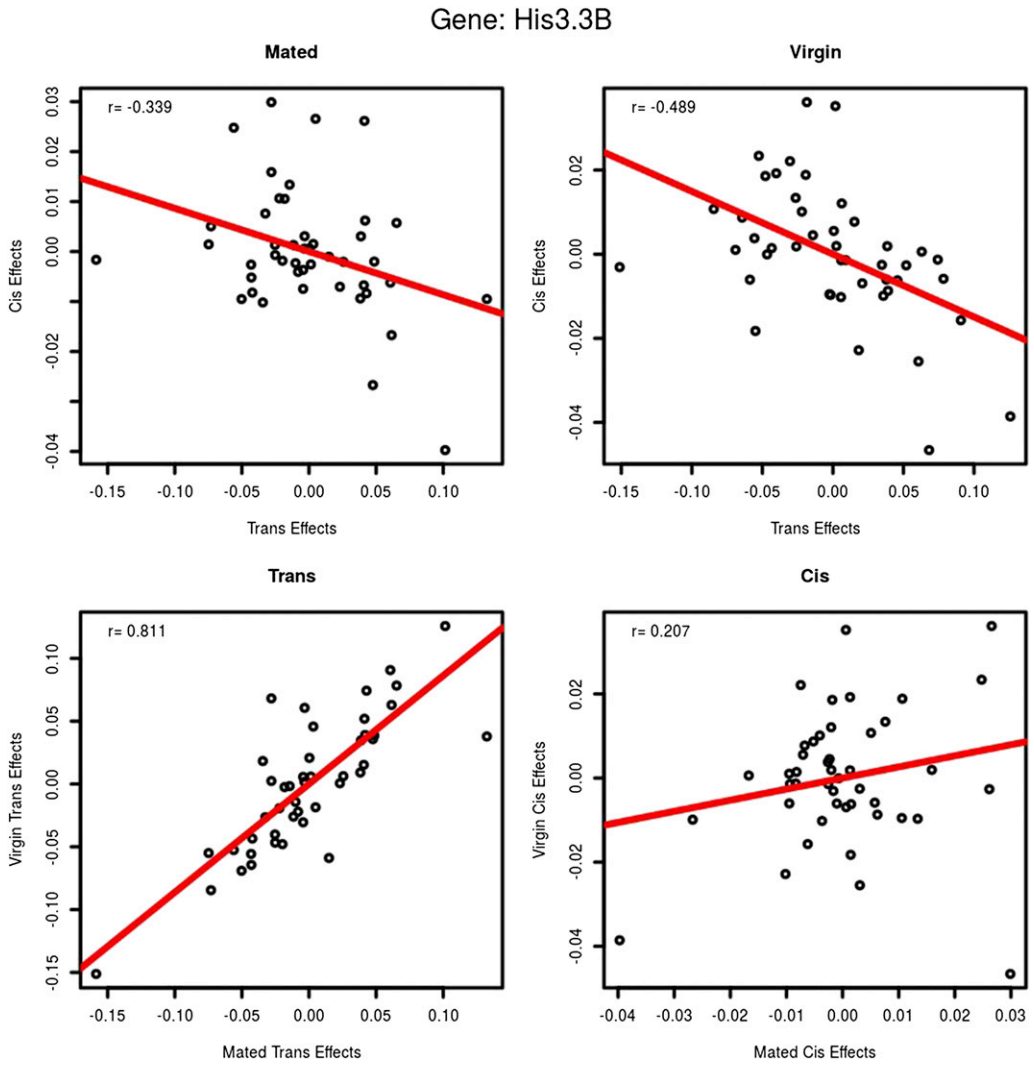

Figure 5 *His3.3B*: *cis*- and *trans*-estimates. This gene was chosen at random as an example to demonstrate how *cis*- and *trans*-effects were compared. Each circle represents one testcross/F_1-hybrid line. The top row compares *cis*- and *trans*-estimates within environment. The *x*-axis is the estimated *trans*-effect and the *y*-axis is the *cis*-effect. *Cis*- and *trans*-effects are negatively correlated for this exon (85% of exons show negative associations in both environments). The bottom row compares *cis*- and *trans*-effects across environments. The *x*-axis is the mated environment and the *y*-axis is the virgin environment. In this example, *trans*-effects are positively associated between mated and virgin flies. *Cis* effects are less correlated in this example but the correlation is positive (99% of all exons are positively correlated for both *cis*- and *trans*-effects across environments with a median correlation of 0.83 for *cis* and 0.95 for *trans*). The red line is the regression. Figure S4 shows the same relationships between *cis*- and *trans*-effects across all crosses and exons.

mating this gene is differentially regulated in virgin but not in mated flies.

There were several genes involved in regulatory regions that were significant for AI in virgin flies only. *Act57B* contributes to developmental processes and cytoskeleton dynamics but has also been shown to play a role in courtship conditioning (Winbush *et al.* 2012). *Kank*, a gene that affects muscle tendon development, has been shown to be differentially expressed downstream of *dsx* (Lebo *et al.* 2009), suggesting AI regulation in the sex determination pathway in virgins only. *p24-1* has sex-specific expression (Boltz *et al.* 2007) and has been shown to play a role in the neural signaling involved in female egg-laying defects and reproductive behavior (Saleem *et al.* 2012). In addition, *ζCOP* is involved in lipid storage and regulation of lipid droplets (Guo *et al.* 2008b) consistent with regulatory changes in lipid metabolism after mating in the fruit fly.

Cis- and trans-effects

We compared all estimates of AI in both environments (Figure 3). AI is largely concordant between environments (Figure 3 and Figure 5), a somewhat surprising result given the magnitude of expression differences reported for these conditions previously (Dalton *et al.* 2010) and in these data (see above) and the presence of ~200 differentially regulated genes. We hypothesize that the large degree of concordance in expression regulation between environments is due to a robust gene regulatory network (Cubillos *et al.* 2014). To explicitly test this hypothesis, we can estimate *cis*- and *trans*-effects for each exon within the population based on the F_1-hybrid tester design (Nuzhdin *et al.* 2012). For exons significant for AI in at least 10 lines ($n = 879$) *cis*- and *trans*-effects were estimated for all lines in mated and virgin conditions separately (Figure 4 and Table S3).

The distribution of estimates (Figure 4, A and B) shows a larger range for *trans*-estimates than for *cis*-estimates. For each exon in mated and virgin environments we calculated the variance of *cis*- and *trans*-estimates (Figure 4, C and D). The variance of *trans*-estimates is much larger than the variance of *cis*-estimates in both environments, consistent with previous studies (Genissel *et al.* 2008). The direction of the estimates for *cis* and *trans* for a particular cross/environment is often different (63%, Table 1) and the association between

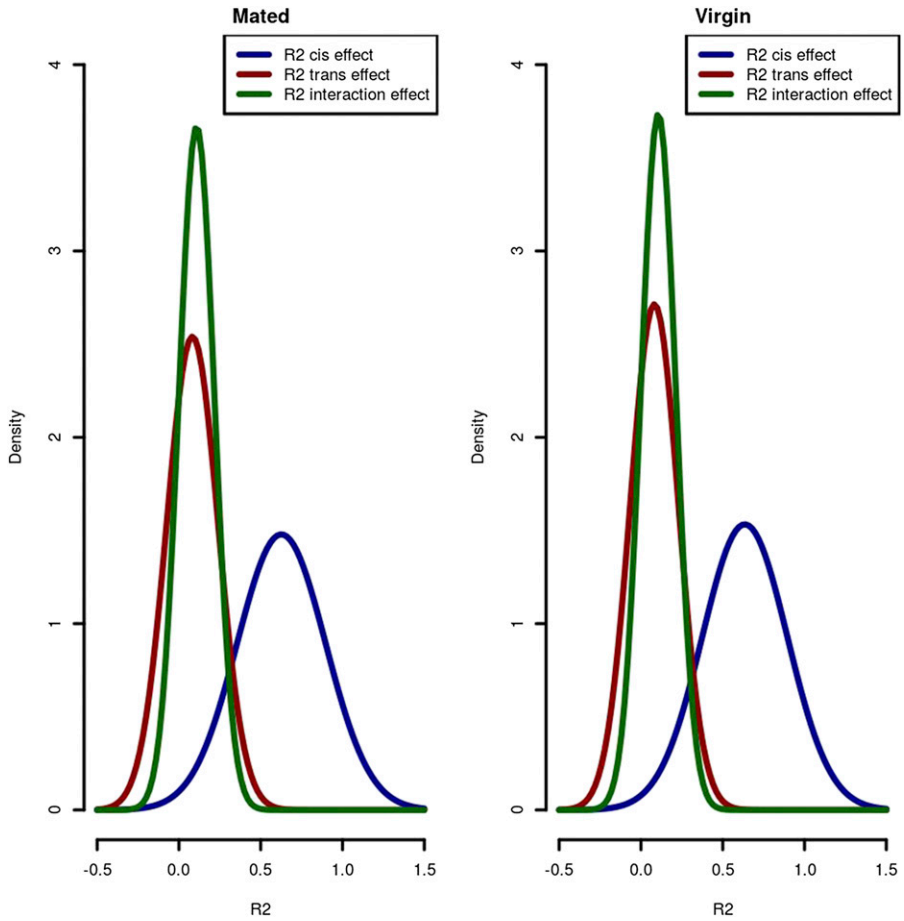

Figure 6 The distribution of R^2 for the regression $Y_{ij} = \mu + C_i + T_i + C_i \times T_i$, where Y is $\hat{\boldsymbol{\theta}}$, C_i is the estimate of *cis*, and T_i is *trans* for line i for each exon j. R^2 is an estimate of the contribution of *cis*-interactions, *trans*-interactions, and *cis*- by *trans*-interactions to AI. Distributions of R^2 are similar in the mated and virgin environments. *Cis*-effects explain at least 45% of the variation in expression for 75% of exons tested. *Trans*-effects explain 8% of the variance on average. The *cis*- by *trans*-interaction explains an additional 11% of the variance on average.

estimates for *cis* and *trans* for a particular exon across crosses is negative 85% of the time (Figure 5, gene *His3.3B*; and Figure S4). In contrast, when comparing *trans*-effects for the same exon across environments the results are strikingly concordant (Figure 5 and Figure S4). *Cis*-effects are likewise similar across environments (Figure 5 and Figure S4).

AI is a result of both *cis* and *trans* and the interaction between them (Figure 1). For each environment we modeled the effect of AI as a function of *cis*- and *trans*-effects and their interaction, using a linear model: $Y_i = \mu + C_i + T_i + C_i \times T_i$, where Y is AI, C_i is the estimate of *cis*, and T_i is *trans* for line i ($i = 1$–n_j). The association between *cis*-effects and AI was nearly always significant. For 75% of the exons tested, *cis*-effects explained at least 45% of the variation in expression (Figure 6 and Table S5). For 25% of exons, *cis*-effects explained >85% of the variance. *Trans*-effects added on average 8% to the proportion of variance explained. We found that 25% of exons had at least 10% of their variance explained by *trans*. Even after accounting for both *cis* and *trans*, the interaction between *cis* and *trans* explains an additional 11% on average. The full model explained at least 40% of the variance for 95% of the exons modeled and 90% of the variance for 50% of the exons (Figure 6, Figure 7, and Table S5).

We identified genes that are regulated completely by *cis* ($R^2 > 0.90$, $n = 170$), have a large *trans*-effect (R^2 due to *trans* >0.40, $n = 50$), or have a large *cis*- by *trans*-interaction effect (R^2 due to the interaction >0.40). Genes regulated primarily by *cis* were enriched for biological Gene Ontology processes involved in centrosome organization ($P = 0.001439$, 12 genes), centrosome cycle ($P < 0.0001$, 11 genes), and centrosome duplication ($P = 0.001839$, 10 genes). In addition, phototransduction ($P = 0.004142$, 8 genes), detection of light stimulus ($P = 0.00949$, 8 genes), response to light stimulus ($P = 0.017$, 11 genes), and detection of visible light ($P = 0.046$, 6 genes) were also enriched. Phototransduction genes are known to be altered by mating in *Drosophila* (Gioti *et al.* 2012; Landis *et al.* 2015).

Of the genes with a large *trans*-effect on AI, *Chmp1* is involved in the negative regulation of the epidermal growth signaling pathway as well as involved in chromatin structure and cell cycle progression (Stauffer *et al.* 2001). *HPS4* is also involved with chromatin, but in the silencing and negative regulation of gene silencing (Lee *et al.* 2009). *jim* is also involved in chromatin silencing (Mugat *et al.* 2015) and PIWI-interacting RNA processes in follicle cells (Saito *et al.* 2009). Finally, *ps* is spliced sex specifically (Telonis-Scott *et al.* 2009) and is a splicing factor (Seshaiah *et al.* 2001) and *Vmat* is involved in transmembrane transport as a splice variant that is involved in dopamine, serotonin, and octopamine transport (Greer *et al.* 2005). Both dopamine signaling and octopamine signaling are implicated in mediating the post-mating response (Rezaval *et al.* 2014; Landis *et al.* 2015).

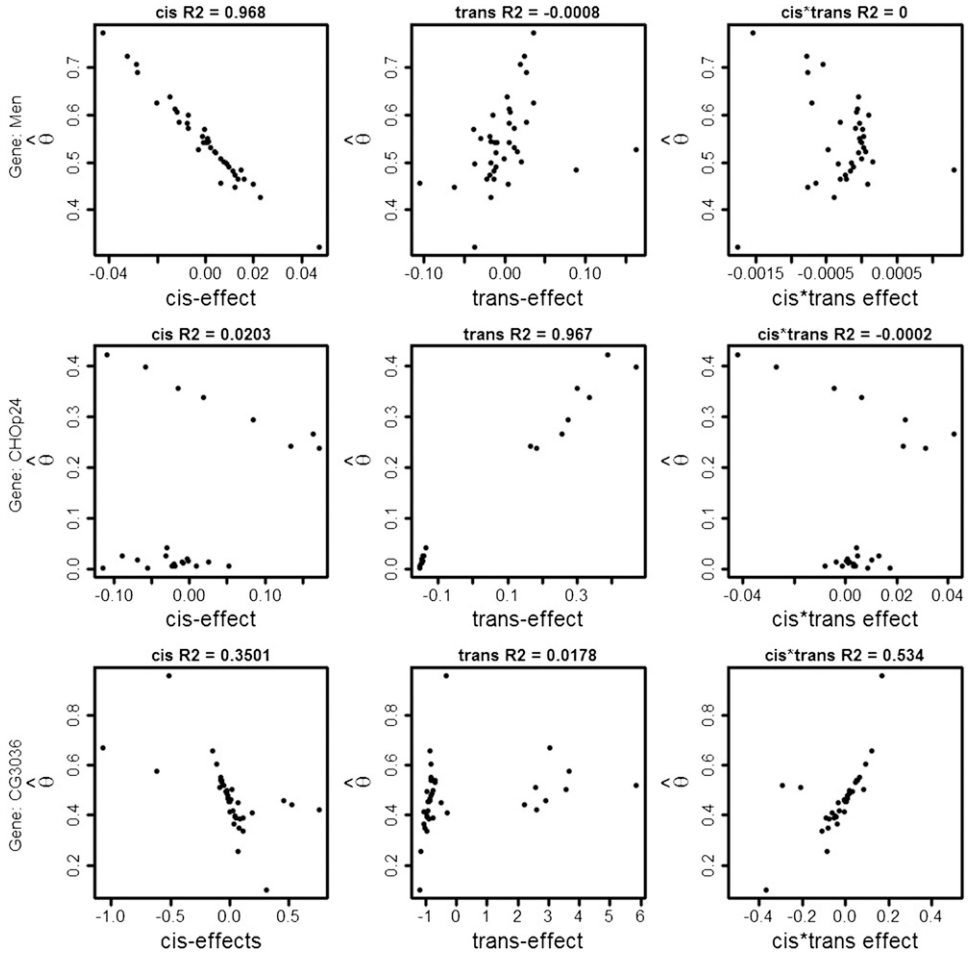

Figure 7 Three exons displaying different patterns of association between *cis*-interactions, *trans*-interactions, and *cis*- by *trans*-interactions and $\hat{\boldsymbol{\theta}}$. Each point is a testcross/F_1 hybrid. On the *y*-axis is the estimated AI ($\hat{\boldsymbol{\theta}}$) and on the *x*-axis in left, center, and right columns are *cis*, *trans*, and *cis* by *trans*. The top row represents the gene Men. This gene has ~97% of the variance explained by the *cis*-effect and a negative association between *cis* and AI. The middle row represents the gene CHOp24. This gene has ~97% of the variance explained by *trans*-effects. The bottom row represents the gene CG3036. This gene has ~53% of variance explained by the *cis*- by *trans*-interaction. Figure S3 depicts lack of association between *cis*- and *trans*-effects with $\hat{\boldsymbol{\theta}}$ when all crosses and all exons are considered simultaneously.

Discussion

This study supports previous findings of differences in expression between mated and virgin flies and goes further in identifying ~200 genes with AI differences between environments. Yet, when AI is detected in both environments, it is concordant and *cis*- and *trans*-effects are concordant across the environments. When AI is detected, *cis* is almost always significant and in this first population-scale study of natural variation within a species, *trans*-effects and *cis*- by *trans*-interactions are sizable. *Trans*-effects are evidence of molecular connections across loci and *cis*- by *trans*-interactions are evidence of genetic variation across loci influencing the phenotype of gene expression. In stark contrast to the cis_M–cis_V and $trans_M$–$trans_V$ comparison across environments the *cis*- and *trans*-effects within an environment (cis_M–$trans_M$; cis_V–$trans_V$) are markedly not concordant in this study (Table S6). The *cis/trans* combinations +/+ and −/− are concordant while +/− and −/+ are compensatory. Here 63% of the effects within a line/exon are compensatory and across lines 85% of the associations between *cis*- and *trans*-effects have a negative slope, leaving us with an unambiguous finding of large-scale compensatory effects in expression regulation. Large-scale compensatory effects within the same species are also supported by a recent elegant experimental study in *Caenorhabditis elegans* (Paaby and Rockman 2014).

There is a strong consensus emerging from the analyses of a variety of model organisms: in yeast (Kvitek *et al.* 2008; Artieri and Fraser 2014), fly (Wang *et al.* 2008; Coolon *et al.* 2014, 2015; Graze *et al.* 2014), and mouse (Goncalves *et al.* 2012; Crowley *et al.* 2015; Pinter *et al.* 2015) that *cis*- and *trans*-effects are compensatory. In intraspecific *D. melanogaster* F_1's, compensatory interactions were observed in 79% of cases, and in interspecific *D. simulans/D. sechelia* and *D. melanogaster/D. simulans* crosses, they corresponded to 73% and 87% of cases (see summary in Coolon *et al.* 2014). How does one explain this strong and phylogenetically ubiquitous pattern?

One frequent explanation for compensatory effects is that *trans*- and *cis*-factors coevolve, as there is a stabilizing selection for overall transcript level (Wittkopp *et al.* 2004, 2008b; Landry *et al.* 2005; Graze *et al.* 2009, 2012; Fontanillas *et al.* 2010; Stevenson *et al.* 2013; McManus *et al.* 2014). A neutral *trans*-mutation is envisioned that spreads jointly with a slightly deleterious *cis*-mutation (see Takahasi *et al.* 2011 for a helpful summary). Takahasi *et al.* (2011, p. 15,279) demonstrate via extensive simulation that "compensatory *cis-trans* interactions gradually accumulated over time." Also

of note, in their simulations (Takahasi *et al.* 2011, p. 15,279) "background dependency of relative allelic expression was not observed *within spec*ies." Within species, *cis*- and *trans*-effects cannot coevolve as they are not cotransmitted. In this experiment in *Drosophila* the likelihood of long-range LD in flies accounting for ∼85% compensatory *vs.* ∼15% concordant *cis–trans* combinations is vanishingly small as the scale of this effect is known to be very small (Pool *et al.* 2012). What is then the evolutionary explanation of such compensation within species?

Gene expression evolves under a house-of-cards model of stabilizing selection (Hodgins-Davis *et al.* 2015), maintaining population genetic variation (Jin *et al.* 2001; Gibson and Dworkin 2004; Nuzhdin *et al.* 2004). This variation contributes to phenotypic diversity and is widespread. If instead of thinking about individual loci we focus on gene regulatory networks (GRNs), then logically there must be variation among loci. How then would that variation be measured in the context of *cis*- and *trans*-effects? If each locus contained variation that affected expression at that locus, we would expect a large number of *cis*-effects, as observed here. Yet, GRNs are inherently models of *trans*-effects, as the connections among genes in the pathway are *trans*. For these data a pathway analysis of the virgin environment modeled regulation of the sex hierarchy, using structural equations (Fear *et al.* 2015). This analysis suggested that there were 754 genes that were linked to the core sex hierarchy. We conducted a similar path analysis of the mated environment and found 380 (50%) were in common, suggesting a large overlap in the *trans*-regulation of genes upstream and downstream of the sex hierarchy in both environments.

In thinking about *cis*- and *trans*-effects in the context of a GRN the relative directions of the *cis*- and *trans*-effects must be considered carefully. For example: If an allele 1 in genotype 1 is upregulated due to *cis*-regulatory mutation (+ effect) and there is also a significant *trans*-effect estimated for the same allele, what direction—upregulating or downregulating (− effect)—would it more frequently have? An alternate effect of the allele in *cis* and *trans* suggests that the overall regulation of the GRN is constrained. Compensatory effects of the allele within a GRN may explain widespread observations of GRN robustness.

GRN robustness has been explicitly formulated to account for the prevalence of compensatory *cis–trans* interactions (Denby *et al.* 2012; Bader *et al.* 2015). Denby *et al.* (2012) have proposed that negative feedback controlling the level of RNA expression could be a common mechanism to buffer effects of regulatory variants in yeast. Screening for autoregulated transcription factors in yeast, Denby *et al.* (2012) found ROX1 to be under strong negative feedback. Mutant experiments showed that this negative feedback confers robustness to the expression of ROX1 in the face of naturally occurring allelic variants present in a set of divergent yeast strains. This study demonstrated for a single gene that negative feedback could act as a buffering mechanism for regulatory variants. Bader *et al.* (2015) quantified buffering by feedback against naturally occurring regulatory variants genome-wide to be ∼15%. Note that when buffering arises from feedback, it is not necessary to invoke additional genetic variation across the genome to explain the *trans*-effects.

If GRNs are generally robust, they have implications in human health research. Analysis of the structure of GRNs in the K562 cancer cell line suggests poor buffering compared to the noncancer cell line GM12878 (Albergante *et al.* 2014). Most of the genome-wide association study associations are between noncoding regions and disease (reviewed in Zhang and Lupski 2015). One potential explanation is that genes are misregulated in disease (reviewed in Lee and Young 2013). As GRN robustness should buffer against misregulation, it implies that disease may be a result of lack of effective buffering. This may make the hunt for genes underlying disease a little more straightforward, as rather than looking for direct links with phenotype, lack of robust regulation can be used to identify potential candidate pathways.

Acknowledgments

We thank Jeremy Newman for his help in the revisions. We thank the editor and anonymous reviewers for insightful comments. This work was supported by National Institutes of Health (NIH) grants GMS102227 (to L.M.M. and S.V.N.), R01MH091561 (to S.V.N. and L.M.M.), 5P50HG002790 (to S.V.N. and J.T.), and AG011833 (to J.T.). The contents of this article are solely the responsibility of the authors and do not necessarily represent the official views of the NIH.

Literature Cited

Albergante, L., J. J. Blow, and T. J. Newman, 2014 Buffered qualitative stability explains the robustness and evolvability of transcriptional networks. eLife 3: e02863.

Anders, S., A. Reyes, and W. Huber, 2012 Detecting differential usage of exons from RNA-seq data. Genome Res. 22: 2008–2017.

Artieri, C. G., and H. B. Fraser, 2014 Evolution at two levels of gene expression in yeast. Genome Res. 24: 411–421.

Bader, D. M., S. Wilkening, G. Lin, M. M. Tekkedil, K. Dietrich *et al.*, 2015 Negative feedback buffers effects of regulatory variants. Mol. Syst. Biol. 11: 785.

Barone, M. C., G. P. Sykiotis, and D. Bohmann, 2011 Genetic activation of Nrf2 signaling is sufficient to ameliorate neurodegenerative phenotypes in a Drosophila model of Parkinson's disease. Dis. Model. Mech. 4: 701–707.

Benjamini, Y., and Y. Hochberg, 1995 Controlling the false discovery rate: a practical and powerful approach to multiple testing. J. R. Stat. Soc. B 57: 289–300.

Berger, R. L., 1997 Likelihood Ratio Tests and Intersection-Union Tests, pp. 225–237 in *Advances in Statistical Decision Theory and Applications*, edited by S. Panchapakesan and N. Balakrishnan. Birkhäuser Boston, Boston, MA.

Berger, R. L., and D. D. Boos, 1999 Confidence limits for the onset and duration of treatment effect. Biom. J. 41: 517–531.

Boltz, K. A., L. L. Ellis, and G. E. Carney, 2007 Drosophila melanogaster p24 genes have developmental, tissue-specific, and sex-specific expression patterns and functions. Dev. Dyn. 236: 544–555.

Brem, R. B., G. Yvert, R. Clinton, and L. Kruglyak, 2002 Genetic dissection of transcriptional regulation in budding yeast. Science 296: 752–755.

Campo, D., K. Lehmann, C. Fjeldsted, T. Souaiaia, J. Kao *et al.*, 2013 Whole-genome sequencing of two North American Drosophila melanogaster populations reveals genetic differentiation and positive selection. Mol. Ecol. 22: 5084–5097.

Castel, S. E., A. Levy-Moonshine, P. Mohammadi, E. Banks, and T. Lappalainen, 2015 Tools and best practices for data processing in allelic expression analysis. Genome Biol. 16: 195.

Chapman, T., L. F. Liddle, J. M. Kalb, M. F. Wolfner, and L. Partridge, 1995 Cost of mating in Drosophila melanogaster females is mediated by male accessory gland products. Nature 373: 241–244.

Coffman, C. J., R. W. Doerge, M. L. Wayne, and L. M. McIntyre, 2003 Intersection tests for single marker QTL analysis can be more powerful than two marker QTL analysis. BMC Genet. 4: 10.

Coolon, J. D., C. J. McManus, K. R. Stevenson, B. R. Graveley, and P. J. Wittkopp, 2014 Tempo and mode of regulatory evolution in Drosophila. Genome Res. 24: 797–808.

Coolon, J. D., K. R. Stevenson, C. J. McManus, B. Yang, B. R. Graveley *et al.*, 2015 Molecular mechanisms and evolutionary processes contributing to accelerated divergence of gene expression on the Drosophila X chromosome. Mol. Biol. Evol. 32: 2605–2615.

Cowles, C. R., J. N. Hirschhorn, D. Altshuler, and E. S. Lander, 2002 Detection of regulatory variation in mouse genes. Nat. Genet. 32: 432–437.

Crowley, J. J., V. Zhabotynsky, W. Sun, S. Huang, I. K. Pakatci *et al.*, 2015 Analyses of allele-specific gene expression in highly divergent mouse crosses identifies pervasive allelic imbalance. Nat. Genet. 47: 353–360.

Cubillos, F. A., O. Stegle, C. Grondin, M. Canut, S. Tisne *et al.*, 2014 Extensive cis-regulatory variation robust to environmental perturbation in Arabidopsis. Plant Cell 26: 4298–4310.

Dalton, J. E., T. S. Kacheria, S. R. Knott, M. S. Lebo, A. Nishitani *et al.*, 2010 Dynamic, mating-induced gene expression changes in female head and brain tissues of Drosophila melanogaster. BMC Genomics 11: 541.

Degner, J. F., J. C. Marioni, A. A. Pai, J. K. Pickrell, E. Nkadori *et al.*, 2009 Effect of read-mapping biases on detecting allele-specific expression from RNA-sequencing data. Bioinformatics 25: 3207–3212.

Denby, C. M., J. H. Im, R. C. Yu, C. G. Pesce and R. B. Brem, 2012 Negative feedback confers mutational robustness in yeast transcription factor regulation. Proc. Natl. Acad. Sci. USA 109: 3874–3878.

Emerson, J. J., L. C. Hsieh, H. M. Sung, T. Y. Wang, C. J. Huang *et al.*, 2010 Natural selection on cis and trans regulation in yeasts. Genome Res. 20: 826–836.

Fear, J. M., M. N. Arbeitman, M. P. Salomon, J. E. Dalton, J. Tower *et al.*, 2015 The Wright stuff: reimagining path analysis reveals novel components of the sex determination hierarchy in Drosophila melanogaster. BMC Syst. Biol. 9: 1.

Flatt, T., 2011 Survival costs of reproduction in Drosophila. Exp. Gerontol. 46: 369–375.

Fontanillas, P., C. R. Landry, P. J. Wittkopp, C. Russ, J. D. Gruber *et al.*, 2010 Key considerations for measuring allelic expression on a genomic scale using high-throughput sequencing. Mol. Ecol. 19: 212–227.

Frith, M. C., R. Wan, and P. Horton, 2010 Incorporating sequence quality data into alignment improves DNA read mapping. Nucleic Acids Res. 38: e100.

Genissel, A., L. M. McIntyre, M. L. Wayne, and S. V. Nuzhdin, 2008 Cis and trans regulatory effects contribute to natural variation in transcriptome of Drosophila melanogaster. Mol. Biol. Evol. 25: 101–110.

Gibson, G., and I. Dworkin, 2004 Uncovering cryptic genetic variation. Nat. Rev. Genet. 5: 681–690.

Gilad, Y., S. A. Rifkin, and J. K. Pritchard, 2008 Revealing the architecture of gene regulation: the promise of eQTL studies. Trends Genet. 24: 408–415.

Gioti, A., S. Wigby, B. Wertheim, E. Schuster, P. Martinez *et al.*, 2012 Sex peptide of Drosophila melanogaster males is a global regulator of reproductive processes in females. Proc. Biol. Sci. 279: 4423–4432.

Goncalves, A., S. Leigh-Brown, D. Thybert, K. Stefflova, E. Turro *et al.*, 2012 Extensive compensatory cis-trans regulation in the evolution of mouse gene expression. Genome Res. 22: 2376–2384.

Graze, R. M., L. M. McIntyre, B. J. Main, M. L. Wayne and S. V. Nuzhdin, 2009 Regulatory divergence in *Drosophila melanogaster* and *D. simulans*, a genome-wide analysis of allele-specific expression. Genetics 183: 547–561.

Graze, R. M., L. L. Novelo, V. Amin, J. M. Fear, G. Casella *et al.*, 2012 Allelic imbalance in Drosophila hybrid heads: exons, isoforms, and evolution. Mol. Biol. Evol. 29: 1521–1532.

Graze, R. M., L. M. McIntyre, A. M. Morse, B. M. Boyd, S. V. Nuzhdin *et al.*, 2014 What the X has to do with it: differences in regulatory variability between the sexes in Drosophila simulans. Genome Biol. Evol. 6: 818–829.

Greer, C. L., A. Grygoruk, D. E. Patton, B. Ley, R. Romero-Calderon *et al.*, 2005 A splice variant of the Drosophila vesicular monoamine transporter contains a conserved trafficking domain and functions in the storage of dopamine, serotonin, and octopamine. J. Neurobiol. 64: 239–258.

Guichet, A., F. Peri, and S. Roth, 2001 Stable anterior anchoring of the oocyte nucleus is required to establish dorsoventral polarity of the Drosophila egg. Dev. Biol. 237: 93–106.

Guo, M., S. Yang, M. Rupe, B. Hu, D. R. Bickel *et al.*, 2008a Genome-wide allele-specific expression analysis using Massively Parallel Signature Sequencing (MPSS) reveals cis- and trans-effects on gene expression in maize hybrid meristem tissue. Plant Mol. Biol. 66: 551–563.

Guo, Y., T. C. Walther, M. Rao, N. Stuurman, G. Goshima *et al.*, 2008b Functional genomic screen reveals genes involved in lipid-droplet formation and utilization. Nature 453: 657–661.

Hodgins-Davis, A., D. P. Rice, and J. P. Townsend, 2015 Gene expression evolves under a house-of-cards model of stabilizing selection. Mol. Biol. Evol. 32: 2130–2140.

Huang, W., M. A. Carbone, M. M. Magwire, J. A. Peiffer, R. F. Lyman *et al.*, 2015 Genetic basis of transcriptome diversity in *Drosophila melanogaster*. Proc. Natl. Acad. Sci. USA 112: E6010–E6019.

Hughes, K. A., J. F. Ayroles, M. M. Reedy, J. M. Drnevich, K. C. Rowe *et al.*, 2006 Segregating variation in the transcriptome: *cis* regulation and additivity of effects. Genetics 173: 1347–1355.

Hutter, S., S. S. Saminadin-Peter, W. Stephan, and J. Parsch, 2008 Gene expression variation in African and European populations of Drosophila melanogaster. Genome Biol. 9: R12.

Jin, W., R. M. Riley, R. D. Wolfinger, K. P. White, G. Passador-Gurgel *et al.*, 2001 The contributions of sex, genotype and age to transcriptional variance in Drosophila melanogaster. Nat. Genet. 29: 389–395.

Karim, M. R., H. Taniguchi, and A. Kobayashi, 2015 Constitutive activation of Drosophila CncC transcription factor reduces lipid formation in the fat body. Biochem. Biophys. Res. Commun. 463: 693–698.

King, E. G., C. M. Merkes, C. L. McNeil, S. R. Hoofer, S. Sen *et al.*, 2012 Genetic dissection of a model complex trait using the Drosophila Synthetic Population Resource. Genome Res. 22: 1558–1566.

King, E. G., B. J. Sanderson, C. L. McNeil, A. D. Long, and S. J. Macdonald, 2014 Genetic dissection of the Drosophila mela-

nogaster female head transcriptome reveals widespread allelic heterogeneity. PLoS Genet. 10: e1004322.
Kirst, M., C. J. Basten, A. A. Myburg, Z. B. Zeng, and R. R. Sederoff, 2005 Genetic architecture of transcript-level variation in differentiating xylem of a eucalyptus hybrid. Genetics 169: 2295–2303.
Kocher, S. D., F. J. Richard, D. R. Tarpy, and C. M. Grozinger, 2008 Genomic analysis of post-mating changes in the honey bee queen (Apis mellifera). BMC Genomics 9: 232.
Kurmangaliyev, Y. Z., A. V. Favorov, N. M. Osman, K. V. Lehmann, D. Campo *et al.*, 2015 Natural variation of gene models in Drosophila melanogaster. BMC Genomics 16: 198.
Kvitek, D. J., J. L. Will, and A. P. Gasch, 2008 Variations in stress sensitivity and genomic expression in diverse S. cerevisiae isolates. PLoS Genet. 4: e1000223.
Landis, G. N., M. P. Salomon, D. Keroles, N. Brookes, T. Sekimura *et al.*, 2015 The progesterone antagonist mifepristone/RU486 blocks the negative effect on life span caused by mating in female Drosophila. Aging 7: 53–69.
Landry, C. R., P. J. Wittkopp, C. H. Taubes, J. M. Ranz, A. G. Clark *et al.*, 2005 Compensatory *cis–trans* evolution and the dysregulation of gene expression in interspecific hybrids of *Drosophila*. Genetics 171: 1813–1822.
Langmead, B., C. Trapnell, M. Pop, and S. L. Salzberg, 2009 Ultrafast and memory-efficient alignment of short DNA sequences to the human genome. Genome Biol. 10: R25.
Lawniczak, M. K., and D. J. Begun, 2004 A genome-wide analysis of courting and mating responses in Drosophila melanogaster females. Genome 47: 900–910.
Lawniczak, M. K., A. I. Barnes, J. R. Linklater, J. M. Boone, S. Wigby *et al.*, 2007 Mating and immunity in invertebrates. Trends Ecol. Evol. 22: 48–55.
Lebo, M. S., L. E. Sanders, F. Sun, and M. N. Arbeitman, 2009 Somatic, germline and sex hierarchy regulated gene expression during Drosophila metamorphosis. BMC Genomics 10: 80.
Lee, T. I., and R. A. Young, 2013 Transcriptional regulation and its misregulation in disease. Cell 152: 1237–1251.
Lee, Y. S., S. Pressman, A. P. Andress, K. Kim, J. L. White *et al.*, 2009 Silencing by small RNAs is linked to endosomal trafficking. Nat. Cell Biol. 11: 1150–1156.
Lemos, B., L. O. Araripe, P. Fontanillas, and D. L. Hartl, 2008 Dominance and the evolutionary accumulation of *cis*- and *trans*-effects on gene expression. Proc. Natl. Acad. Sci. USA 105: 14471–14476.
Leon-Novelo, L. G., L. M. McIntyre, J. M. Fear, and R. M. Graze, 2014 A flexible Bayesian method for detecting allelic imbalance in RNA-seq data. BMC Genomics 15: 920.
Lo, H. S., Z. Wang, Y. Hu, H. H. Yang, S. Gere *et al.*, 2003 Allelic variation in gene expression is common in the human genome. Genome Res. 13: 1855–1862.
Mack, P. D., A. Kapelnikov, Y. Heifetz, and M. Bender, 2006 Mating-responsive genes in reproductive tissues of female *Drosophila melanogaster*. Proc. Natl. Acad. Sci. USA 103: 10358–10363.
Mackay, T. F., E. A. Stone, and J. F. Ayroles, 2009 The genetics of quantitative traits: challenges and prospects. Nat. Rev. Genet. 10: 565–577.
Mackay, T. F., S. Richards, E. A. Stone, A. Barbadilla, J. F. Ayroles *et al.*, 2012 The Drosophila melanogaster Genetic Reference Panel. Nature 482: 173–178.
Massouras, A., S. M. Waszak, M. Albarca-Aguilera, K. Hens, W. Holcombe *et al.*, 2012 Genomic variation and its impact on gene expression in Drosophila melanogaster. PLoS Genet. 8: e1003055.
McGraw, L. A., G. Gibson, A. G. Clark, and M. F. Wolfner, 2004 Genes regulated by mating, sperm, or seminal proteins in mated female Drosophila melanogaster. Curr. Biol. 14: 1509–1514.
McGraw, L. A., A. G. Clark, and M. F. Wolfner, 2008 Postmating gene expression profiles of female *Drosophila melanogaster* in response to time and to four male accessory gland proteins. Genetics 179: 1395–1408.
McManus, C. J., J. D. Coolon, M. O. Duff, J. Eipper-Mains, B. R. Graveley *et al.*, 2010 Regulatory divergence in Drosophila revealed by mRNA-seq. Genome Res. 20: 816–825.
McManus, C. J., J. D. Coolon, J. Eipper-Mains, P. J. Wittkopp, and B. R. Graveley, 2014 Evolution of splicing regulatory networks in Drosophila. Genome Res. 24: 786–796.
Meiklejohn, C. D., J. D. Coolon, D. L. Hartl, and P. J. Wittkopp, 2014 The roles of cis- and trans-regulation in the evolution of regulatory incompatibilities and sexually dimorphic gene expression. Genome Res. 24: 84–95.
Mendell, J. T., and H. C. Dietz, 2001 When the message goes awry: disease-producing mutations that influence mRNA content and performance. Cell 107: 411–414.
Michalak, P., and M. A. Noor, 2003 Genome-wide patterns of expression in Drosophila pure species and hybrid males. Mol. Biol. Evol. 20: 1070–1076.
Michalak, P., and M. A. Noor, 2004 Association of misexpression with sterility in hybrids of Drosophila simulans and D. mauritiana. J. Mol. Evol. 59: 277–282.
Misra, J. R., M. A. Horner, G. Lam, and C. S. Thummel, 2011 Transcriptional regulation of xenobiotic detoxification in Drosophila. Genes Dev. 25: 1796–1806.
Morrow, E. H., and P. Innocenti, 2012 Female postmating immune responses, immune system evolution and immunogenic males. Biol. Rev. Camb. Philos. Soc. 87: 631–638.
Mugat, B., A. Akkouche, V. Serrano, C. Armenise, B. Li *et al.*, 2015 MicroRNA-dependent transcriptional silencing of transposable elements in Drosophila follicle cells. PLoS Genet. 11: e1005194.
Munger, S. C., N. Raghupathy, K. Choi, A. K. Simons, D. M. Gatti *et al.*, 2014 RNA-Seq alignment to individualized genomes improves transcript abundance estimates in multiparent populations. Genetics 198: 59–73.
Nothnagel, M., A. Wolf, A. Herrmann, K. Szafranski, I. Vater *et al.*, 2011 Statistical inference of allelic imbalance from transcriptome data. Hum. Mutat. 32: 98–106.
Nuzhdin, S. V., M. L. Wayne, K. L. Harmon, and L. M. McIntyre, 2004 Common pattern of evolution of gene expression level and protein sequence in Drosophila. Mol. Biol. Evol. 21: 1308–1317.
Nuzhdin, S. V., M. L. Friesen, and L. M. McIntyre, 2012 Genotype-phenotype mapping in a post-GWAS world. Trends Genet. 28: 421–426.
Obata, F., and M. Miura, 2015 Enhancing S-adenosyl-methionine catabolism extends Drosophila lifespan. Nat. Commun. 6: 8332.
Ortiz-Barrientos, D., B. A. Counterman, and M. A. Noor, 2007 Gene expression divergence and the origin of hybrid dysfunctions. Genetica 129: 71–81.
Paaby, A. B., and M. V. Rockman, 2014 Cryptic genetic variation: evolution's hidden substrate. Nat. Rev. Genet. 15: 247–258.
Pastinen, T., 2010 Genome-wide allele-specific analysis: insights into regulatory variation. Nat. Rev. Genet. 11: 533–538.
Peng, J., P. Zipperlen, and E. Kubli, 2005 Drosophila sex-peptide stimulates female innate immune system after mating via the Toll and Imd pathways. Curr. Biol. 15: 1690–1694.
Pickering, A. M., T. A. Staab, J. Tower, D. Sieburth, and K. J. Davies, 2013 A conserved role for the 20S proteasome and Nrf2 transcription factor in oxidative stress adaptation in mammals, Caenorhabditis elegans and Drosophila melanogaster. J. Exp. Biol. 216: 543–553.

Pinter, S. F., D. Colognori, B. J. Beliveau, R. I. Sadreyev, B. Payer *et al.*, 2015 Allelic imbalance is a prevalent and tissue-specific feature of the mouse transcriptome. Genetics 200: 537–549.

Pool, J. E., R. B. Corbett-Detig, R. P. Sugino, K. A. Stevens, C. M. Cardeno *et al.*, 2012 Population genomics of sub-Saharan Drosophila melanogaster: African diversity and non-African admixture. PLoS Genet. 8: e1003080.

Ranz, J. M., K. Namgyal, G. Gibson, and D. L. Hartl, 2004 Anomalies in the expression profile of interspecific hybrids of Drosophila melanogaster and Drosophila simulans. Genome Res. 14: 373–379.

Rezaval, C., T. Nojima, M. C. Neville, A. C. Lin, and S. F. Goodwin, 2014 Sexually dimorphic octopaminergic neurons modulate female postmating behaviors in Drosophila. Curr. Biol. 24: 725–730.

Rockman, M. V., and L. Kruglyak, 2006 Genetics of global gene expression. Nat. Rev. Genet. 7: 862–872.

Ronald, J., J. M. Akey, J. Whittle, E. N. Smith, G. Yvert *et al.*, 2005 Simultaneous genotyping, gene-expression measurement, and detection of allele-specific expression with oligonucleotide arrays. Genome Res. 15: 284–291.

Rozowsky, J., A. Abyzov, J. Wang, P. Alves, D. Raha *et al.*, 2011 AlleleSeq: analysis of allele-specific expression and binding in a network framework. Mol. Syst. Biol. 7: 522.

Saito, K., S. Inagaki, T. Mituyama, Y. Kawamura, Y. Ono *et al.*, 2009 A regulatory circuit for piwi by the large Maf gene traffic jam in Drosophila. Nature 461: 1296–1299.

Saleem, S., C. C. Schwedes, L. L. Ellis, S. T. Grady, R. L. Adams *et al.*, 2012 Drosophila melanogaster p24 trafficking proteins have vital roles in development and reproduction. Mech. Dev. 129: 177–191.

Seshaiah, P., B. Miller, M. M. Myat, and D. J. Andrew, 2001 pasilla, the Drosophila homologue of the human Nova-1 and Nova-2 proteins, is required for normal secretion in the salivary gland. Dev. Biol. 239: 309–322.

Skelly, D. A., M. Johansson, J. Madeoy, J. Wakefield, and J. M. Akey, 2011 A powerful and flexible statistical framework for testing hypotheses of allele-specific gene expression from RNA-seq data. Genome Res. 21: 1728–1737.

Smith, E. N., and L. Kruglyak, 2008 Gene-environment interaction in yeast gene expression. PLoS Biol. 6: e83.

Smith, G., Y. Fang, X. Liu, J. Kenny, A. R. Cossins *et al.*, 2013 Transcriptome-wide expression variation associated with environmental plasticity and mating success in cactophilic Drosophila mojavensis. Evolution 67: 1950–1963.

Springer, N. M., and R. M. Stupar, 2007 Allele-specific expression patterns reveal biases and embryo-specific parent-of-origin effects in hybrid maize. Plant Cell 19: 2391–2402.

Stauffer, D. R., T. L. Howard, T. Nyun, and S. M. Hollenberg, 2001 CHMP1 is a novel nuclear matrix protein affecting chromatin structure and cell-cycle progression. J. Cell Sci. 114: 2383–2393.

Stell, R., J. Torrie, and D. Dickey, 1980 *Principles and Procedures of Statistics: A Biometrical Approach*. MacGraw-Hill, New York.

Stevenson, K. R., J. D. Coolon, and P. J. Wittkopp, 2013 Sources of bias in measures of allele-specific expression derived from RNA-sequence data aligned to a single reference genome. BMC Genomics 14: 536.

Sykiotis, G. P., I. G. Habeos, A. V. Samuelson, and D. Bohmann, 2011 The role of the antioxidant and longevity-promoting Nrf2 pathway in metabolic regulation. Curr. Opin. Clin. Nutr. Metab. Care 14: 41–48.

Takahasi, K. R., T. Matsuo, and T. Takano-Shimizu-Kouno, 2011 Two types of *cis-trans* compensation in the evolution of transcriptional regulation. Proc. Natl. Acad. Sci. USA 108: 15276–15281.

Telonis-Scott, M., A. Kopp, M. L. Wayne, S. V. Nuzhdin, and L. M. McIntyre, 2009 Sex-specific splicing in *Drosophila*: widespread occurrence, tissue specificity and evolutionary conservation. Genetics 181: 421–434.

Tirosh, I., S. Reikhav, A. A. Levy, and N. Barkai, 2009 A yeast hybrid provides insight into the evolution of gene expression regulation. Science 324: 659–662.

Trapnell, C., D. G. Hendrickson, M. Sauvageau, L. Goff, J. L. Rinn *et al.*, 2013 Differential analysis of gene regulation at transcript resolution with RNA-seq. Nat. Biotechnol. 31: 46–53.

van de Geijn, B., G. McVicker, Y. Gilad, and J. Pritchard, 2015 WASP: allele-specific software for robust discovery of molecular quantitative trait loci. Nat. Methods 12: 1061–1063.

Wang, H.-Y., Y. Fu, M. S. McPeek, X. Lu, S. Nuzhdin *et al.*, 2008 Complex genetic interactions underlying expression differences between *Drosophila* races: analysis of chromosome substitutions. Proc. Natl. Acad. Sci. USA 105: 6362–6367.

Wayne, M. L., Y. J. Pan, S. V. Nuzhdin, and L. M. McIntyre, 2004 Additivity and *trans*-acting effects on gene expression in male *Drosophila simulans*. Genetics 168: 1413–1420.

Wayne, M. L., M. Telonis-Scott, L. M. Bono, L. Harshman, A. Kopp *et al.*, 2007 Simpler mode of inheritance of transcriptional variation in male *Drosophila melanogaster*. Proc. Natl. Acad. Sci. USA 104: 18577–18582.

Winbush, A., D. Reed, P. L. Chang, S. V. Nuzhdin, L. C. Lyons *et al.*, 2012 Identification of gene expression changes associated with long-term memory of courtship rejection in *Drosophila* males. G3 2: 1437–1445.

Wittkopp, P. J., and G. Kalay, 2012 Cis-regulatory elements: molecular mechanisms and evolutionary processes underlying divergence. Nat. Rev. Genet. 13: 59–69.

Wittkopp, P. J., B. K. Haerum, and A. G. Clark, 2004 Evolutionary changes in cis and trans gene regulation. Nature 430: 85–88.

Wittkopp, P. J., B. K. Haerum, and A. G. Clark, 2006 Parent-of-origin effects on mRNA expression in *Drosophila melanogaster* not caused by genomic imprinting. Genetics 173: 1817–1821.

Wittkopp, P. J., B. K. Haerum, and A. G. Clark, 2008a Independent effects of *cis*- and *trans*-regulatory variation on gene expression in *Drosophila melanogaster*. Genetics 178: 1831–1835.

Wittkopp, P. J., B. K. Haerum, and A. G. Clark, 2008b Regulatory changes underlying expression differences within and between Drosophila species. Nat. Genet. 40: 346–350.

Yan, H., W. Yuan, V. E. Velculescu, B. Vogelstein, and K. W. Kinzler, 2002 Allelic variation in human gene expression. Science 297: 1143.

Yasuyama, K., T. Kitamoto, and P. M. Salvaterra, 1995 Immunocytochemical study of choline acetyltransferase in Drosophila melanogaster: an analysis of cis-regulatory regions controlling expression in the brain of cDNA-transformed flies. J. Comp. Neurol. 361: 25–37.

Yuan, S., and Z. Qin, 2012 Read-mapping using personalized diploid reference genome for RNA sequencing data reduced bias for detecting allele-specific expression. IEEE Int. Conf. Bioinform. Biomed. Workshops 2012: 718–724.

Zhang, F., and J. R. Lupski, 2015 Non-coding genetic variants in human disease. Hum. Mol. Genet. 24: R102–R110.

Zhang, X., and J. O. Borevitz, 2009 Global analysis of allele-specific expression in *Arabidopsis thaliana*. Genetics 182: 943–954.

Zhou, S., T. Mackay, and R. R. Anholt, 2014 Transcriptional and epigenetic responses to mating and aging in Drosophila melanogaster. BMC Genomics 15: 927.

Zou, F., W. Sun, J. J. Crowley, V. Zhabotynsky, P. F. Sullivan *et al.*, 2014 A novel statistical approach for jointly analyzing RNA-Seq data from F_1 reciprocal crosses and inbred lines. Genetics 197: 389–399.

Communicating editor: J. A. Birchler

GENETICS

Supporting Information
www.genetics.org/lookup/suppl/doi:10.1534/genetics.116.188797/-/DC1

Buffering of Genetic Regulatory Networks in *Drosophila melanogaster*

Justin M. Fear, Luis G. León-Novelo, Alison M. Morse, Alison R. Gerken, Kjong Van Lehmann, John Tower, Sergey V. Nuzhdin, and Lauren M. McIntyre

DOI: 10.1534/genetics.116.188797

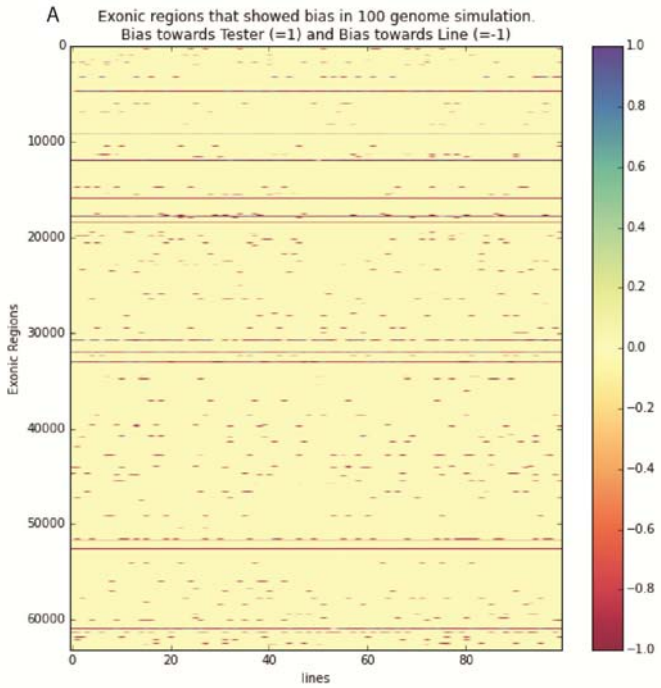
A
Exonic regions that showed bias in 100 genome simulation.
Bias towards Tester (=1) and Bias towards Line (=-1)
Exonic Regions
lines
0
10000
20000
30000
40000
50000
60000
0
20
40
60
80
1.0
0.8
0.6
0.4
0.2
0.0
−0.2
−0.4
−0.6
−0.8
−1.0

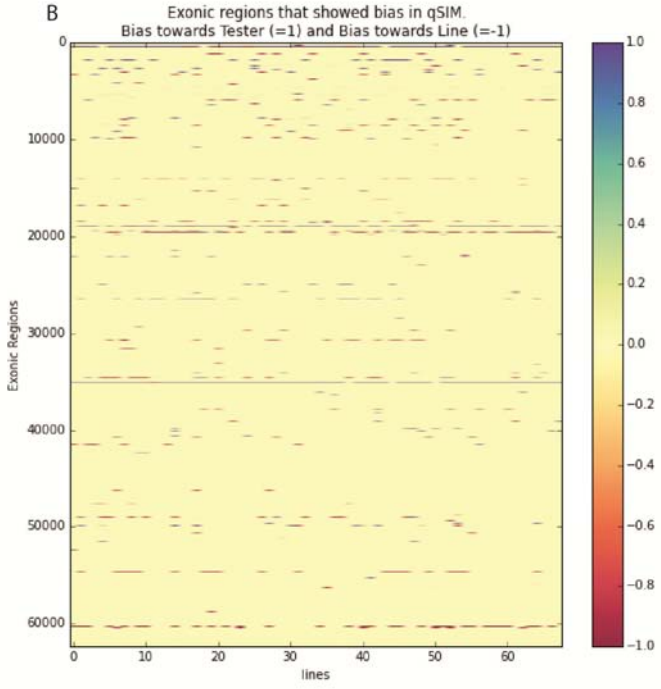
B
Exonic regions that showed bias in qSIM.
Bias towards Tester (=1) and Bias towards Line (=-1)
Exonic Regions
lines
0
10000
20000
30000
40000
50000
60000
0
10
20
30
40
50
60
1.0
0.8
0.6
0.4
0.2
0.0
−0.2
−0.4
−0.6
−0.8
−1.0

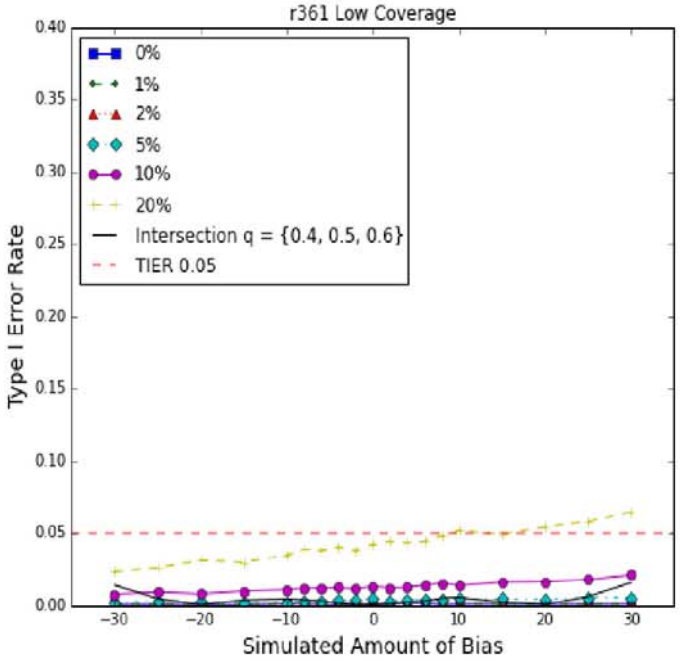
r361 Low Coverage
0%
1%
2%
5%
10%
20%
Intersection q = {0.4, 0.5, 0.6}
TIER 0.05
Type I Error Rate
Simulated Amount of Bias

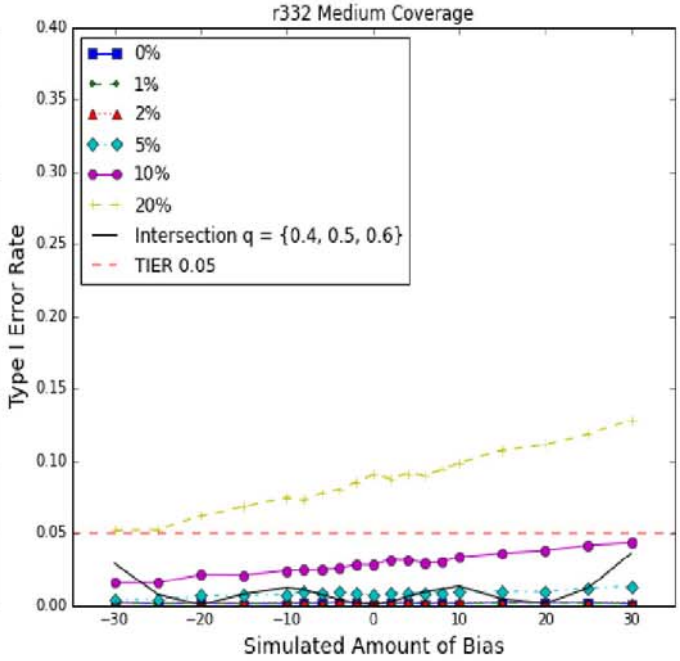
r332 Medium Coverage
0%
1%
2%
5%
10%
20%
Intersection q = {0.4, 0.5, 0.6}
TIER 0.05
Type I Error Rate
Simulated Amount of Bias

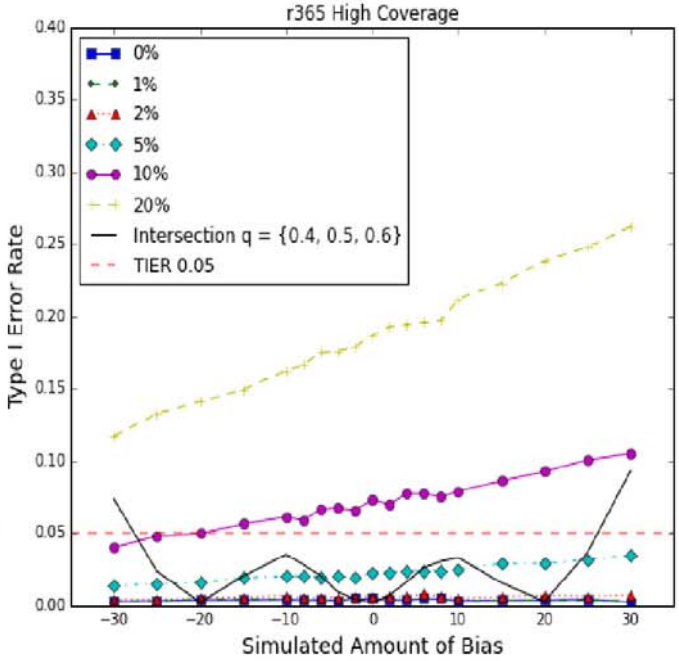
r365 High Coverage
0%
1%
2%
5%
10%
20%
Intersection q = {0.4, 0.5, 0.6}
TIER 0.05
Type I Error Rate
Simulated Amount of Bias

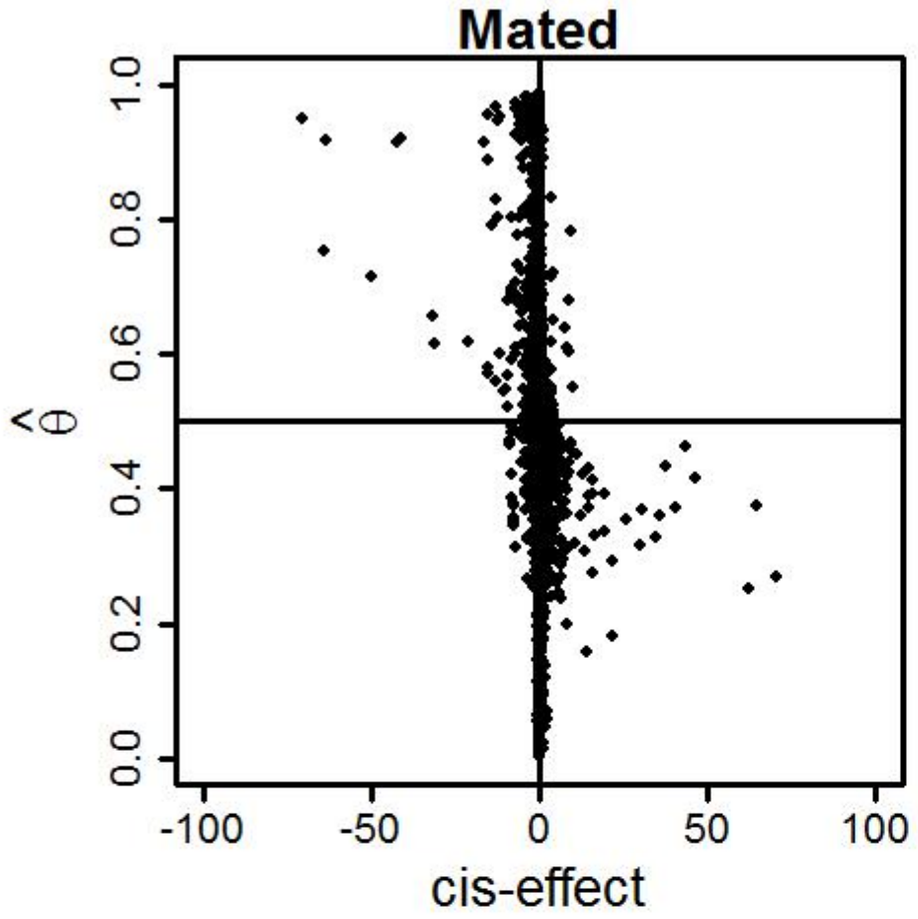
Mated
$\hat{\theta}$
0.0
0.2
0.4
0.6
0.8
1.0
-100
-50
0
50
100
cis-effect

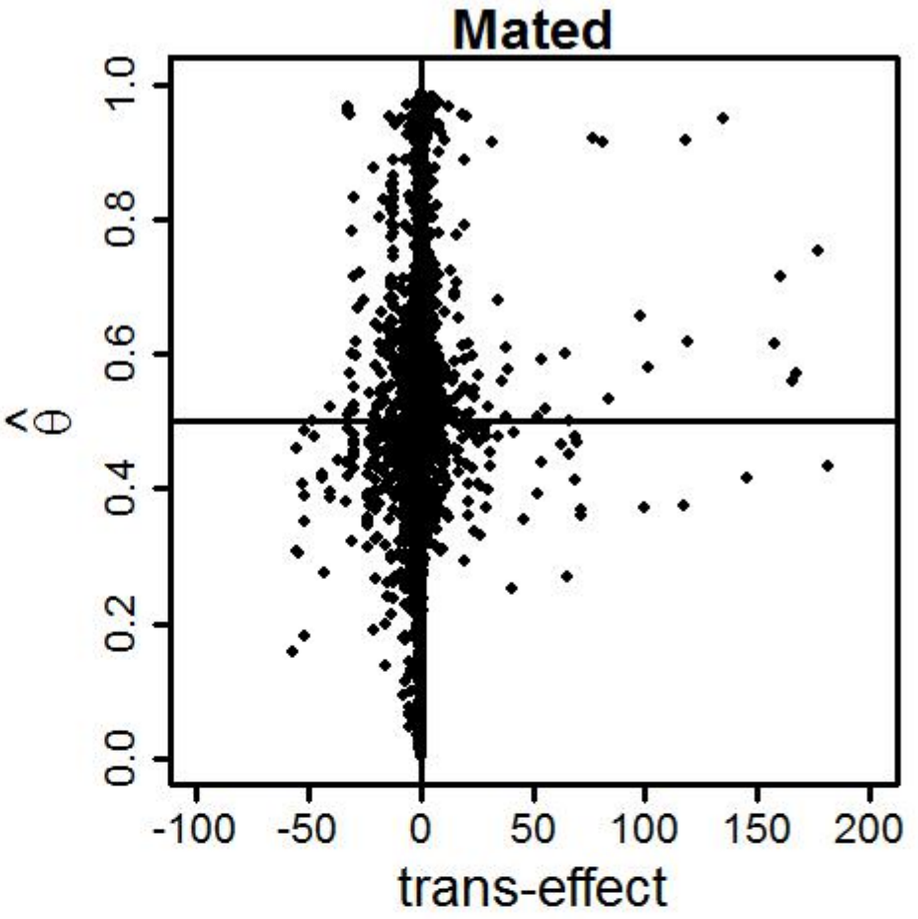
Mated
$\hat{\theta}$
0.0
0.2
0.4
0.6
0.8
1.0
-100
-50
0
50
100
150
200
trans-effect

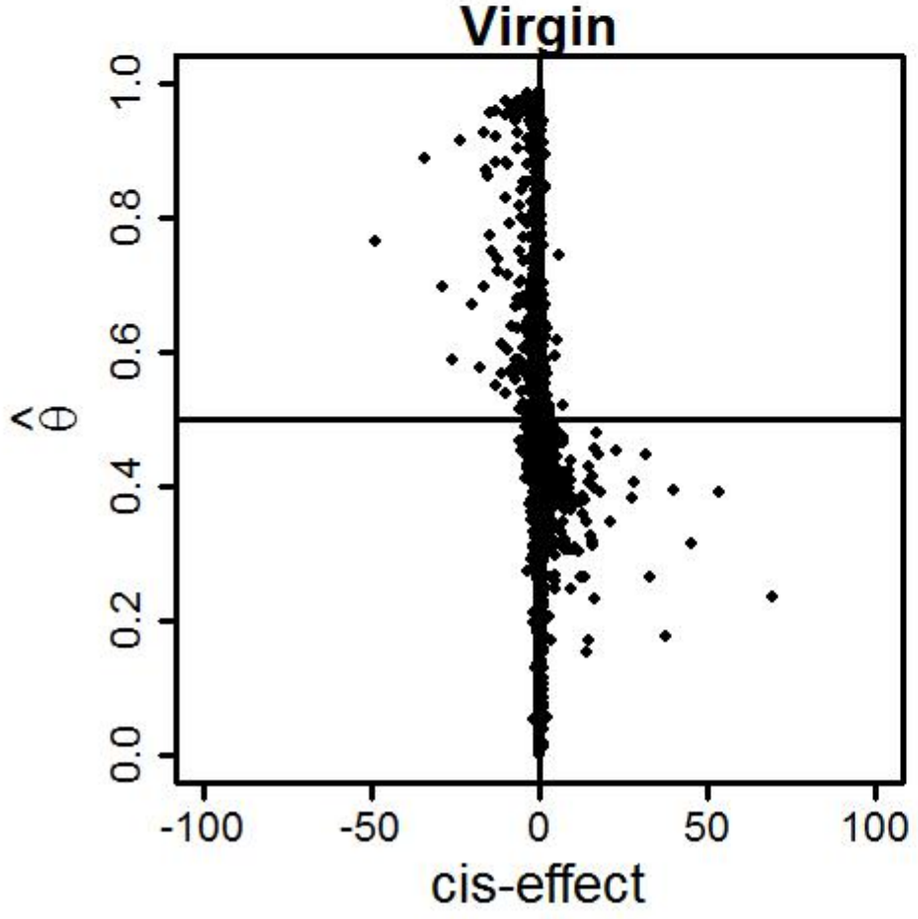
Virgin
$\hat{\theta}$
0.0
0.2
0.4
0.6
0.8
1.0
-100
-50
0
50
100
cis-effect

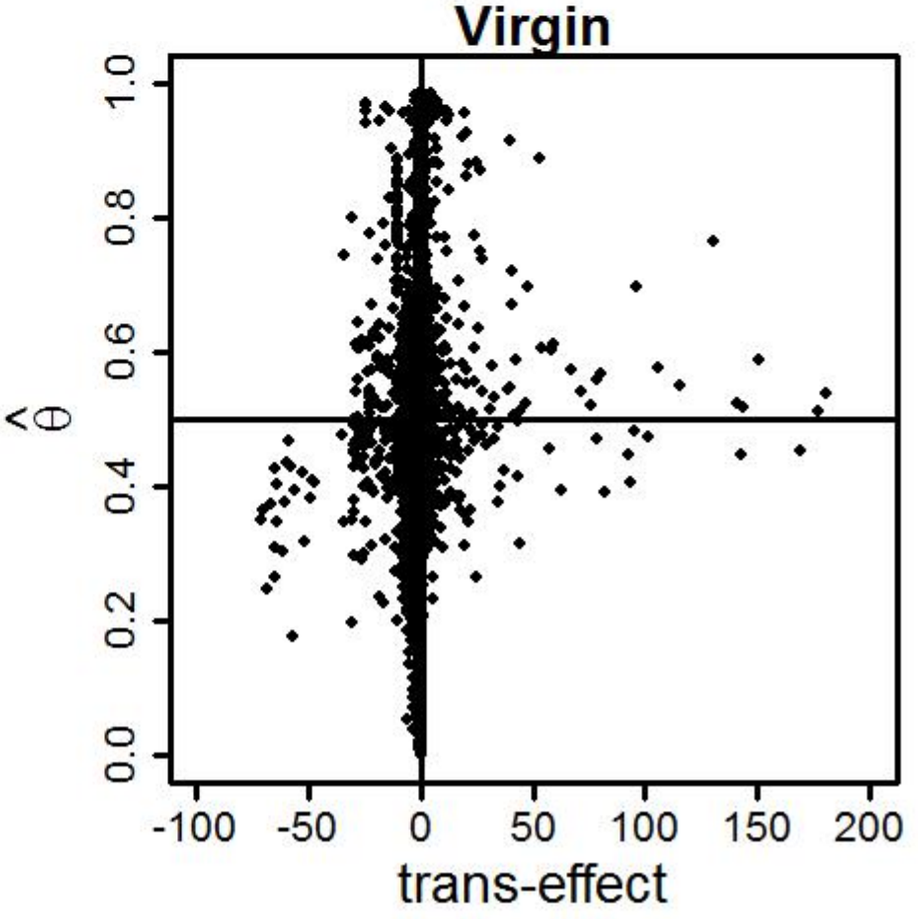
Virgin
$\hat{\theta}$
0.0
0.2
0.4
0.6
0.8
1.0
-100
-50
0
50
100
150
200
trans-effect

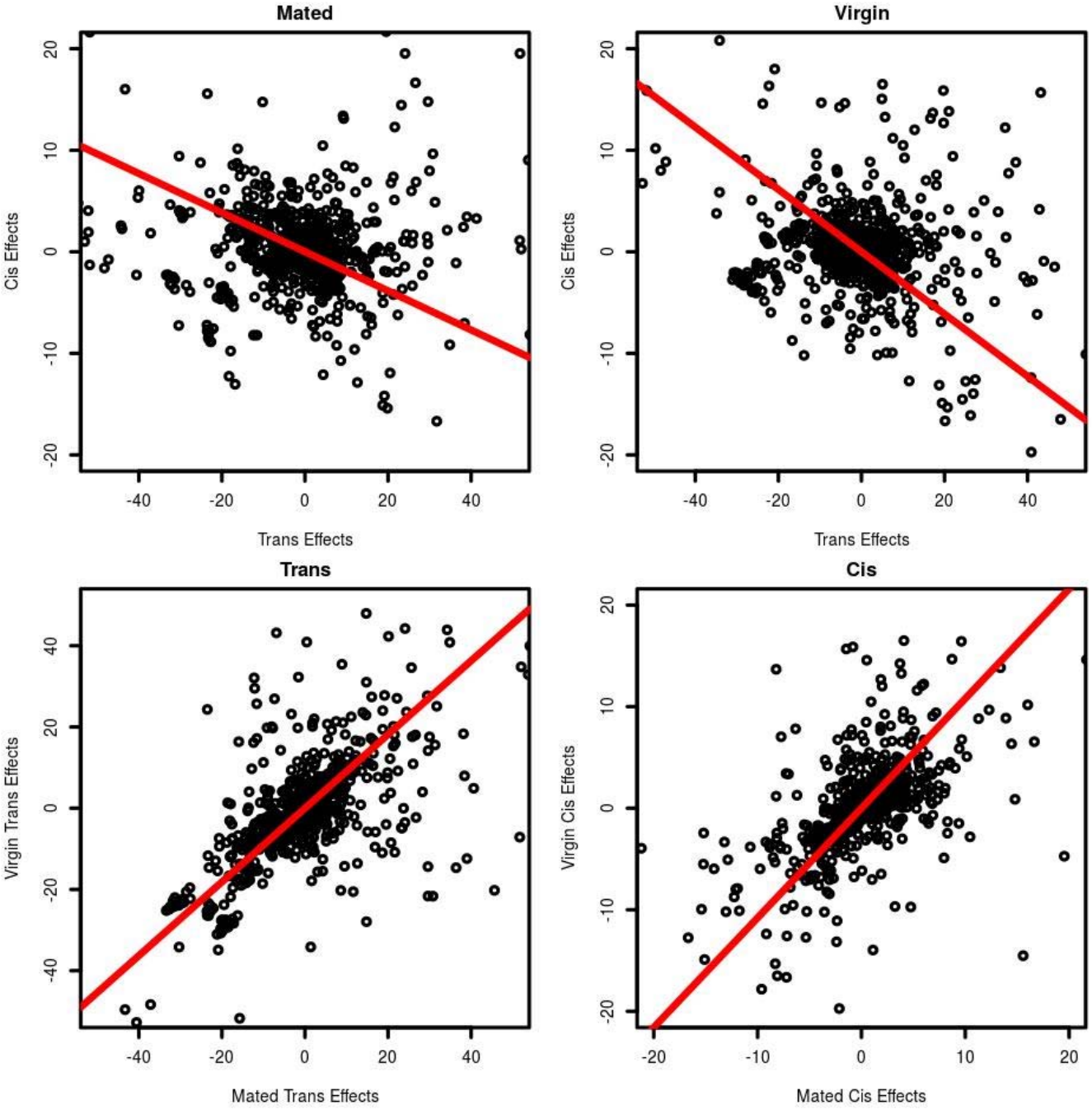
Mated
Cis Effects
Trans Effects
Virgin
Cis Effects
Trans Effects
Trans
Virgin Trans Effects
Mated Trans Effects
Cis
Virgin Cis Effects
Mated Cis Effects

Table S1. Exons that show genome ambiguity in simulations with random snps or genome ambiguity from simulations based on snps for that line (qsim). (.zip, 1 KB)

Available for download as a .zip file at
www.genetics.org/lookup/suppl/doi:10.1534/genetics.116.188797 /-/DC1/TableS1.zip

Table S2. Allelic imbalance (AI) is underrepresented in exons with low coverage. Exons were equally binned into twenty categories of expression. Exons in the low category show a depletion of allelic imbalance calls (p-value < 0.0001).

Mean APN Range	AB	AI	Total	Percent
0 < APN < 0.29	95447	1425	96872	1.47
0.29 ≤ APN < 0.59	92461	4334	96795	4.48
0.59 ≤ APN < 0.94	89905	6861	96766	7.09
0.94 ≤ APN < 1.36	87946	8866	96812	9.16
1.36 ≤ APN < 1.84	86444	10376	96820	10.72
1.84 ≤ APN < 2.39	85039	11784	96823	12.17
2.39 ≤ APN < 3.01	84125	12694	96819	13.11
3.01 ≤ APN < 3.72	83415	13364	96779	13.81
3.72 ≤ APN < 4.55	83001	13819	96820	14.27
4.55 ≤ APN < 5.50	82440	14364	96804	14.84
5.50 ≤ APN < 6.63	82594	14231	96825	14.70
6.63 ≤ APN < 8	83309	14500	97809	14.83
8 ≤ APN < 9.67	81834	14017	95851	14.62
9.67 ≤ APN < 11.81	82570	14217	96787	14.69
11.81 ≤ APN < 14.63	82508	14271	96779	14.75
14.63 ≤ APN < 18.64	82802	14009	96811	14.47
18.64 ≤ APN < 24.81	82948	13863	96811	14.32
24.81 ≤ APN < 36	82861	13954	96815	14.41
36 ≤ APN < 65.83	81495	15312	96807	15.82
65.83 ≤ APN	72268	24542	96810	25.35
Total	1685412	250803	1936215	12.95

Table S3. Table of analyzed exonic regions with associated gene names, *cis* and *trans* effects calculated, mean AI, and counts. (.zip, 4,150 KB)

Available for download as a .zip file at
www.genetics.org/lookup/suppl/doi:10.1534/genetics.116.188797 /-/DC1/TableS3.zip

Table S4. Genes that are significant for AI in mating only, virgin only. (.zip, 2 KB)

Available for download as a .zip file at
www.genetics.org/lookup/suppl/doi:10.1534/genetics.116.188797 /-/DC1/TableS4.zip

Table S5. Regression of *cis* and *trans* and *cis-by-trans* interaction effects on AI. (.zip, 3 KB)

Available for download as a .zip file at
www.genetics.org/lookup/suppl/doi:10.1534/genetics.116.188797 /-/DC1/TableS5.zip

Table S6. Correlations between cis and trans effects. (.zip, 77 KB)

Available for download as a .zip file at
www.genetics.org/lookup/suppl/doi:10.1534/genetics.116.188797 /-/DC1/TableS6.zip

File S1. A filtered VCF used to create genotype specific exome references.

A zipped set of files can be downloaded here:

http://bio.rc.ufl.edu/pub/mcintyre/papers/fear_ase_2016/ase_lvl2_filtered_vcf_files/lvl2_filtered_vcf_files.tgz

File S2. Raw data for allele specific expression analysis. (.zip, 2,144 KB)

Available for download as a .zip file at

www.genetics.org/lookup/suppl/doi:10.1534/genetics.116.188797 /-/DC1/FileS2.zip

Programs: http://github.com/McIntyre-Lab/papers/tree/master/fear_ase_2016

Figures

Figure S1: A) Heat map of the exons that show bias in a simulation of 100 genomes. Bias toward the line (genotype) is indicated by red coloration, bias toward the tester (w1118) is indicated by blue. Yellow coloration means there is low or no bias. There are 807 exons that show bias in all 100 simulated F1 hybrids. These are removed from further analysis. B) Heat map of exons that show bias in qSIM data used to estimate allelic imbalance. A total of 4,634 regions were biased toward the tester allele (blue) and 5,709 regions were biased toward the genotype allele (red). A total of 252 regions had bias in at least half of the line-tester combinations.

Figure S2. Effects of misspecification and coverage on type I error. A simulation was used to estimate type I error with different levels of misspecification at different levels of coverage. The distribution of coverage was based on data from three representative crosses. On the X axis is the simulated amount of bias and on the Y axis is the estimated type I error rate. Note that 10% of .01 is smaller than 10% of .99 and so the amount of bias simulated increases with the proportion. Colored lines represent different amounts of misspecification. As misspecification increases, the type I error rate increases (colored lines in each panel). Control of the type I error rate of 0.05 (dashed red line) is maintained for most cases. At low coverage even a 20% misspecification of bias still results in a type I error rate less than the nominal level. Type I error control is lost when misspecification is high and coverage is high.

Figure S3. The relationship between AI and *cis* and *trans* effects across all exons and crosses. Each point is a single exon for a single line. $\hat{\theta}$ is on the Y axis and the estimate of c*is* or *trans* is on the X axis. The top panels are the mated environment and the bottom panels are the virgin environment. There is no association between *cis* and *trans* effects and $\hat{\theta}$ when crosses and exons are considered simultaneously. This shows that high estimates of AI do not necessarily produce low estimates of *cis*. Relationships between c*is*, *trans* and *cis* by *trans* interactions and $\hat{\theta}$ are strong within each exon. Figure 8 shows three genes as an example of the relationship between AI and *cis* and *trans* effects within an exon.

Figure S4. c*is* and *trans* estimates for all exons with significant AI. The top panels show negative association between *cis* and *trans* effects for both mated and virgin environments. The bottom panels show positive association of *cis* effects and *trans* effects across environments. This suggests that flies in the mated and virgin environments are similar in their *cis* and *trans* regulation. The red line is a linear regression.

Tables

Table S1: Exons that show genome ambiguity in simulations with random snps or genome ambiguity from simulations based on snps for that line (qsim). A value of 1 means

the exon is biased; a 0 value means that it is not biased in the simulation. qsim, was only estimated for exons not universally biased in the random simulation.

Table S2. Allelic imbalance (AI) is underrepresented in exons with low coverage. Exons were equally binned into twenty categories of expression. Exons in the low category show a depletion of allelic imbalance calls (p-value < 0.0001).

Mean APN Range	AB	AI	Total	Percent
0 < APN < 0.29	95447	1425	96872	1.47
0.29 ≤ APN < 0.59	92461	4334	96795	4.48
0.59 ≤ APN < 0.94	89905	6861	96766	7.09
0.94 ≤ APN < 1.36	87946	8866	96812	9.16
1.36 ≤ APN < 1.84	86444	10376	96820	10.72
1.84 ≤ APN < 2.39	85039	11784	96823	12.17
2.39 ≤ APN < 3.01	84125	12694	96819	13.11
3.01 ≤ APN < 3.72	83415	13364	96779	13.81
3.72 ≤ APN < 4.55	83001	13819	96820	14.27
4.55 ≤ APN < 5.50	82440	14364	96804	14.84
5.50 ≤ APN < 6.63	82594	14231	96825	14.70
6.63 ≤ APN < 8	83309	14500	97809	14.83
8 ≤ APN < 9.67	81834	14017	95851	14.62
9.67 ≤ APN < 11.81	82570	14217	96787	14.69
11.81 ≤ APN < 14.63	82508	14271	96779	14.75
14.63 ≤ APN < 18.64	82802	14009	96811	14.47
18.64 ≤ APN < 24.81	82948	13863	96811	14.32
24.81 ≤ APN < 36	82861	13954	96815	14.41
36 ≤ APN < 65.83	81495	15312	96807	15.82
65.83 ≤ APN	72268	24542	96810	25.35
Total	1685412	250803	1936215	12.95

Table S3: Table of analyzed exonic regions with associated gene names, *cis* and *trans* effects calculated, mean AI, and counts. *Cis* and *trans* effects were calculated when there were at least 10 lines at a given exonic region for the combination of mated and virgin treatments. The column “analyze_cis_effects” indicates whether or not the exonic region was analyzed for *cis* and *trans* effects; 1 = analyzed, 0 = not analyzed. For columns of tests of AI (AI_intersection_test, AI_qsim_test, AI_intersection_qsim_both), 1= there was AI detected in this test and 0= there was no AI detected in this test. Column “flag_AI_alternate_direction” is 1 when exons within the gene that have AI both >0.5 and <0.5. These differences across genes may be due to isoform usage.

Table S4: Genes that are significant for AI in mating only, virgin only.

Table S5 Regression of *cis* and *trans* and *cis-by-trans* interaction effects on AI. R2 values for the estimates of the contributions of each effect on AI are given. Models were named as follows AI=cis+trans+cis*trans is the full model. AI=cis+trans is the noint model. AI=cis is the cis model. R2 of the interaction effect was estimated as R2_diff_int=R2_full-R2_noint; R2 of the trans effect was estimated as R2_diff_trans=R2_noint-R2_cis.

Table S6: Correlations between cis and trans effects. Cis_corr is the correlation across environments between the cis effects, trans_corr is the correlation across environments of the trans effects. If cis_corr>0 then direction_cis_corr="+"; if trans_corr>0 then direction_trans_corr="+"; abs_cis/trans_corr is the absolute value of the correlation coefficient. Ct_mated_corr is the correlation of cis and trans effects in the mated environment. Ct_virgin_corr is the correlation of cis and trans effects in the virgin environment. if ct_mated_corr>0 then direction_ct_mated_corr="+"; if ct_virgin_corr>0 then direction_ct_virgin_corr="+";

Data Files

File S1: A filtered VCF used to create genotype specific exome references. A zipped set of files can be downloaded here: http://bio.rc.ufl.edu/pub/mcintyre/papers/fear_ase_2016/ase_lvl2_filtered_vcf_files/lvl2_filtered_vcf_files.tgz

File S2: Raw data for allele specific expression analysis. Columns are: line, mating_status, exonic region LINE_TOTAL_1 LINE_TOTAL_2 LINE_TOTAL_3 LINE_TOTAL_4 LINE_TOTAL_5 LINE_TOTAL_6 TESTER_TOTAL_1 TESTER_TOTAL_2 TESTER_TOTAL_3 TESTER_TOTAL_4 TESTER_TOTAL_5 TESTER_TOTAL_6 flag_analyze